UNCLASSIFIED

ANL-5257(Del.)

ARGONNE NATIONAL LABORATORY
P. O. Box 299
Lemont, Illinois

March 31, 1954

QUARTERLY REPORT
JANUARY, FEBRUARY, AND MARCH 1954

Frank G. Foote, Director
James F. Schumar, Associate Director

METALLURGY DIVISION

Previous Quarterly Reports:

ANL-5234 October, November, December, 1953 (Not Issued)
ANL-5153 July, August, September, 1953
ANL-5097 April, May, June, 1953

Operated by The University of Chicago
under
Contract W-31-109-eng-38

UNCLASSIFIED

TABLE OF CONTENTS

TABLE OF CONTENTS

QUARTERLY REPORT
JANUARY, FEBRUARY, AND MARCH 1954
METALLURGY DIVISION

ABSTRACT

I. Water Cooled Reactors

Uranium-zirconium-niobium alloys containing 5 w/o Zr + 1.5 w/o Nb were cast into Zircaloy II, with bonding at the interface between the casting and can appearing to be quite good. A casting of this type was rolled at 850°C from 1.232" to 0.320" with no evidence of bond rupture, but with some lack of uniformity in clad thickness.

II. Liquid Metal Cooled Reactors

Eighteen of the fast exponential fuel plates have been prepared by inert arc welding; the development work is now complete and the procedure is being taught to shop personnel.

Work on the manufacture of a new fuel charge for EBR has been completed. The fuel slugs are centrifugally cast enriched uranium- 2 w/o zirconium alloy; the fuel blanket slugs are natural uranium-2 w/o zirconium alloy, rolled and heat treated for stability under irradiation.

III. Reactor Development Metallurgy

Melting and casting techniques for producing binary and ternary uranium alloys have been investigated; uranium-zirconium, uranium-niobium, and uranium-zirconium-niobium were studied. The solution of niobium in uranium is a function of time, temperature and agitation; once in solution, niobium does not segregate in the ingot. Segregation of zirconium in the ternary alloys was noticed. Life of high purity magnesia crucibles was very poor when used in preparing the ternary alloys, every crucible cracking after its removal from the furnace.

Corrosion and thermal conductivity tests have been made on zirconium and titanium base alloys. Zr-4% Al, Zr-7% Ti, tested in static degassed water at 360°C exhibited very poor corrosion resistance in a short-term test; Ti-8% Al in static, air-saturated water at 360°C exhibited excellent corrosion resistance over a two-month test.

Thermal conductivities of these alloys at about 45°C were:

Zr-4% Al	0.020 cal/cm²/sec/°C/cm
Zr-7% Ti	0.031 cal/cm²/sec/°C/cm
Ti-8% Al	0.022 cal/cm²/sec/°C/cm

IV. Basic Metallurgy

Work on determining the self-diffusion coefficient of uranium using U^{235} tracer has started. Preliminary tests indicate the cathodic sputtering of specially prepared surface in purified argon at low pressure will be a satisfactory method of forming the diffusion interface.

The compressive deformation characteristics of eleven additional single crystals of alpha uranium have been studied. In many of these crystals the axis of compression was so chosen as to minimize slip on (010) planes in the [100] direction and to enhance slip on $(1\bar{1}0)$ planes in a [110] direction. Despite these favorable conditions, slip on $(1\bar{1}0)$ planes was not observed in any of the crystals. Instead, deformation was by slip on (010) planes or by twinning on (130) planes or (172) planes. One crystal was orientated in such a way as to encourage twinning on $\{176\}$ planes. However, deformation occurred primarily by slip on the (010) plane. In several crystals, orientated in such a way as to inhibit slip on (010) plane, cross slip, probably on (001) planes, was observed.

A new series of high purity uranium-carbon alloys containing 110 to 260 ppm carbon have been prepared. Previously prepared alloys containing 250 and 500 ppm carbon have been heat treated at temperatures ranging from 700° to 1100°C. None of these heat treatments completely dissolved the second phase and the tentative conclusion is that the solid solubility of carbon in beta and gamma uranium is less than 250 ppm.

A series of uranium-zirconium alloys containing from 0.09 w/o to 2.5 w/o Zr have been isothermally heat treated at 400° and 500°C for periods ranging from 5 seconds to 5 minutes, followed by a water quench. Holding time at either temperature had no effect on the resulting microstructure. This strongly suggests that the transformation is complete in less than five seconds at 400° and 500°C. The same structures are obtained by direct quenching from the gamma phase. Up to about 1 w/o Zr the structures consist of coarse grained alpha uranium; above 1% Zr an acicular structure is observed.

A portion of the uranium-zirconium phase diagram in which the epsilon phase occurs has been studied by microscopic and high temperature X-ray methods. At 610°C the X-ray pattern shows only alpha uranium plus alpha zirconium lines. At 600°C and lower, extra lines due to the epsilon

phase are also present. These results suggest that the epsilon phase forms by peritectiod reaction between the terminal solid solutions and that the epsilon phase is not a superstructure based on the gamma phase.

V. Applied Metallurgy

A detailed study of the zone melting process as applied to the purification of uranium is under way. The problem involves the experimental determination of the effective separation factor ($k_{eff.}$) and distinguished from the theoretical factor ($k_{the.}$) obtained from the phase diagram. Factors which cause the effective separation to be less than the theoretical separation are: (1) the diffusion rates of solute in molten and solid uranium; (2) the degree of thermal and magnetic stirring in the molten zone; (3) the irregularity of the solidifying interface; (4) the length of the molten zone; and (5) the rate of motion of the molten zone. The fifth factor (speed of travel of the molten zone) can be varied through wide limits. Single pass experiments at various speeds have been carried out to establish the rates required to move different impurities. In general, it appears that rates of about 1 inch/hour are effective in moving carbon but that a rate of about 0.25 inch/hour is necessary to move metallic impurities such as iron, chromium and nickel. One multiple pass run at a high speed (7.5 inches/hour) reduced the carbon in the leading end of a rod from an initial value of 100 ppm to 20 ppm.

Diffusion coatings of USi_2 on uranium have been produced by immersing uranium specimens in hot NaK alloy containing dissolved silicon metal. Coating thickness increases with increasing silicon concentration temperature and time. Adherent coatings are produced when the variables are adjusted to produce thin coatings. Some improvement in corrosion resistance is shown during the first few hours of test but local attack through pinholes in the coating soon results in undercutting.

Slugs of unalloyed beta treated uranium, 3/8" in diameter and 1" long, were wrapped in zirconium foil and sealed into stainless steel capsules of varying wall thicknesses (0.013" to 0.047"). A free volume of about 6% was allowed within the capsule to allow for thermal and transformation volume changes. After 150 cycles from 100°C to 800°C, i.e., from the alpha phase, through the beta, and into the gamma phase, dimensional changes, measured on the jackets, were less than one per cent in all cases.

Cast U-2 w/o Zr alloys have been examined after burnup up to 2.3%. At this level of burnup the axial elongation was about 6% and the density decrease about 8%. The diameter also increased about the same rate. These changes are explainable in terms of the volume increase associated with the production of additional atoms by the fission process. Unidirectional dimensional changes, characteristic of wrought material, are absent or at least very small in these cast alloys. The specimens remain quite smooth up to burnups of 2.3%.

Preliminary irradiation results have been obtained on U-Zr (1 and 2 w/o Zr) alloys, U-Cr (0.1 and 0.4 w/o Cr) alloys, and unalloyed uranium specimens prepared cooperatively by ANL, BMI and KAPL. The rolled and alpha annealed uranium-zirconium alloys containing 100 to 500 ppm carbon showed a growth rate of 1200 microinches/inch/cycle under thermal cycling, but a shrinkage rate of 150 microinches/inch/ppm burnup after an irradiation of 0.04% BU.

A specimen of gamma quenched uranium-niobium alloy containing 3 w/o Nb was irradiated to a burnup of 0.15%. This specimen elongated under irradiation, indicating that these wrought and heat treated alloys which show good resistance to corrosion by hot water are not stable under even moderate irradiation.

Specimens of the special heat of Type 347 stainless steel used in constructing certain parts of EBR, have been examined after irradiation in EBR up to integrated fast neutron fluxes as high as $2.4 \cdot 10^{20}$ nvt. Plots of tensile strength and Rockwell A hardness versus log (nvt) are linear, showing an increase of 17,000 psi and 4 R_A hardness points per tenfold increase in exposure. No saturation is yet apparent.

VI. Aqueous Corrosion

During the initial stages of corrosion of aluminum in water, it appears that at least one-third of the corrosion product formed in the first half-hour does not remain on the sample surface. This behavior is important in understanding the rather large amount of corrosion which takes place during the initial exposure period, even though the ultimate corrosion rate may be quite low.

Aluminum specimens, corrosion tested at 250° and 275°C in water at pH 3.5 with potassium dichromate and with sodium silicate added as inhibitors, failed by intergranular attack. During the initial stages of intergranular attack, small blisters are formed on the metal surface. It is postulated that hydrogen formed by the corrosion reaction penetrates the metal, diffuses to internal cavities, and separates to form hydrogen gas under pressure. The soft aluminum yields under this pressure and forms a bulge on the surface; when this bulge breaks open, a blister forms which admits water to fresh metal and the whole process is self-accelerating.

Three experiments were run to test this hydrogen blister hypothesis. In one series of experiments, various cations were added to the corroding solution; these plate out on the aluminum surface and form local cathodes on which hydrogen will be liberated. No blisters formed on samples corroded in solutions containing Co, Cd or Ni ions. Another test involves making the specimen anodic to a stainless steel counterelectrode by an externally applied polarizing current. In this case hydrogen is liberated at the counterelectrode and very little blistering of the aluminum occurred. If the potential

is reversed (aluminum made cathodic) severe blistering was observed. A third experiment involved vacuum melting of the aluminum to remove porosity in which hydrogen could accumulate. Such metal showed a low corrosion rate and no blistering.

Further work on the effect of pH on corrosion rate at elevated temperatures has shown the minimum rates are obtained at pH 3 in the temperature range of 200°-300°C.

High purity aluminum specimens, corroded at 160°C in degassed distilled water, fail by blister formation in a few days.

Anodic films of two different thicknesses were applied to zirconium samples. In most cases, the electrical resistivity to the film was independent of the thickness and further the resistivity of the film had little relationship to the corrosion rates of the specimens in water at 300°C.

Two magnesium base alloys [FS-1a, (2.7% Al, 0.3% Mn, 1.0% Zn) and a special AEC high purity alloy (2.7% Al)] were corrosion tested at 90°C in a dynamic system at 17 and 20 feet/second. The test solutions were maintained alkaline at pH 8 to 10 since previous tests had shown that in a static system the corrosion process itself brings the pH to approximately 10. The weight loss-time curves show a constantly increasing slope; after the first ten days the rates were of the order of 15-25 mg/dm^2/day. One test was performed at 150°C under essentially stagnant conditions using pH 10 oxygen-saturated solution. The magnesium had disintegrated by the end of four days.

A sample of unalloyed uranium was heat treated in vacuo for six hours at 1000°C for thorough degassing. The corrosion rate in boiling distilled water was 2.8 mg/cm^2/hour.

Further corrosion testing at 300°C on U-Zr-Nb alloys containing 4.8 w/o Zr and variable amounts of niobium has shown that 1.5 w/o Nb is required and that 2 w/o Nb does not further improve the corrosion resistance. The presence of 300 ppm silicon in these alloys is harmful.

Tests on U-3 w/o Nb alloys containing various additional alloy elements has shown the beneficial effect of tin. In particular, an alloy containing 3 w/o Nb + 0.7% Sn is much more resistant to tempering at 400°C than are the U-3 w/o Nb or the U-5 w/o Si-1.5 w/o Nb alloys.

I. WATER COOLED REACTORS

1. Cast Bonding of Uranium-Zirconium-Niobium Alloy to Zircaloy (J. W. Frank, R. E. Macherey)

The manufacture of fuel elements of uranium rich alloys by picture frame techniques on any large scale would seem to promise enough difficulty to warrant exploration of alternative processes of manufacture.

One avenue of approach to this problem is the casting of uranium or uranium alloys in zirconium or zirconium alloy cans, with or without subsequent fabrication steps. Bennett and Macherey[1] cast unalloyed uranium into a zirconium tube mold and obtained at least partial bonding. Shuck[2] cast Zr-5 w/o U alloy into crystal bar zirconium and into zirconium-tin alloy cans and found, in some experiments, good bonding to the pure zirconium. On the other hand, he reported lack of success with the zirconium-tin alloy cans, presumably due to volatilization of tin from the can during casting. Evans and Allen[3] succeeded in casting the uranium-chromium eutectic alloy around zirconium tubes. Carlson and Armstrong[4] succeeded in casting unalloyed uranium slugs into unalloyed zirconium cans. These were closed without further fabrication steps.

This current series of experiments were aimed at the casting of U-5 w/o Zr-1.5 w/o Nb alloy into relatively short sections of Zircaloy II cladding, relatively thick. It was planned to roll the product to produce approximately 1/4" diameter clad rods closed at one end.

First attempts were with Zircaloy sheet made into 6" half tubes, which were sandblasted and welded by the heliarc process at the two longitudinal seams with argon gas passing through the interior of the tube. A plug was welded in the bottom in the same way. The finished can was about 1-1/4" O.D., 1" I.D. 6" long, and had a 3/8" thick bottom.

---

[1] ANL-4581 (p. 25) ANL Quarterly Progress Report, Metallurgy Division, December 31, 1950.

[2] ANL-5089 "Zrclad Zirconium-Uranium Alloy Rod for Heat Thru-put Test," A. B. Shuck, April 17, 1952.

[3] MIT-1113 Technical Progress Report for the Period April Through June 1953, MIT Metallurgical Project, Issued September 4, 1953.

[4] ISC-426 Ames Quarterly Summary Research Report for the Hanford Slug Program, for July, August and September 1953, Issued November 23, 1953.

This was put into a graphite cylinder bored to 2-1/2" diameter, excepting for about 1" at the bottom where it conformed to the can. Platinum-10% rhodium thermocouples were wired to the top and bottom of the can exterior and the assembly put into a vacuum furnace so that the upper part was relatively near the inductive field. A quantity of U-Zr-Nb alloy scrap was put into a small MgO crucible, which was in turn put into a graphite heater and the assembly placed in the maximum inductive field of the furnace. The furnace was evacuated to a moderate vacuum (0.5 - 1.0 μ) and the uranium alloy melted. The top of the can was at 1000°C, the bottom at 775°C, and the metal at 1325°C when poured. Sectioning showed some bonding but none along any of the welds. A possible explanation, excepting temperature, may lie in the fact that a crevice was left on the inside of all welds. An attempt to break the bond produced failure in the Zircaloy.

The second casting was spoiled by a leaking stopper rod. On the third attempt, the bottom can thermocouple failed. The upper thermocouple showed 1115°C; the metal was at 1390°C by an optical pyrometer. Bonding appeared complete, except at the bottom periphery.

Further tests were made using cans, 1-1/4" O.D., 1" I.D., 6-1/4" long, and with a 3/8" bottom, machined of rolled Zircaloy II rod. Seven castings were made into these cans, with can temperature 940° to 1040°C at the top, 900° to 920°C at the bottom, and liquid alloy at 1400°C. All interfaces appeared to be bonded when the top was cut off, and there was no pipe apparent. The first was cut extensively, after machining slightly eccentrically, so that the interface was penetrated. Bonding at the interface partially machined away, appeared to be very good except for isolated porous areas. A density determination, by weight and measurement, showed 16.8 grams/cm^3, the same as similar measurement on a rolled specimen. Further evidence for bonding was the contraction in the diameter of the Zircaloy can from 1.250" to 1.232" after casting.

The second casting of this type was rolled at 850°C to 0.32" diameter with no evidence of bond rupture. There was some lack of uniformity in clad thickness, particularly in the smaller sections. An internal burst occurred in the core alloy of the first (largest) rolled sample some time after rolling and sectioning. This first rolled specimen differed from the others in diameter and in that it was water quenched from the rolls; all other specimens were reheated to 850°C before water quenching.

II. LIQUID METAL COOLED REACTORS

1. The Welding of Fast Exponential Fuel Plates (C. C. Stone, R. A. Noland)

The fuel plates for the fast exponential experiment consist of a sheet of U^{235} sheathed with natural uranium by the picture frame technique.

Eighteen of a total of 480 fast exponential fuel plates have been inert arc welded at their edges with excellent results. Development work on this program is now completed, and the procedure is being taught to shop personnel who will complete the remainder of the units under the direction of Metallurgy Division personnel. A final report describing this development is now in preparation.

2. Alloy Fuel Charge for EBR (Frank L. Yaggee)

Work on the fabrication of a full set of new fuel rods for the reloading of EBR has been completed. The fuel slugs were centrifugally cast enriched uranium-2 w/o zirconium alloy, the fuel blanket slugs were cast, rolled and heat treated natural uranium-2 w/o zirconium alloy jacketed in thin stainless steel tubes. Two special thermocouple rods were also prepared and shipped to EBR.

III. REACTOR DEVELOPMENT METALLURGY

1. Casting of High Uranium Alloys (J. E. Baird, R. E. Macherey)

The uranium alloys cast during the first quarter of 1954 were U-Nb-Zr, U-Nb and U-Zr. Normal uranium Mallinckrodt biscuits were used for all charges. No premelted biscuit was used in the preparation of these alloys. The zirconium for the 5 kg melts was Grade II crystal bar rolled to 0.020" sheet, while sponge was used for the larger melts. Niobium cubes made from pressed and sintered powder were the only source of niobium.

All 5 kg melts were made in high purity V-2 magnesia crucibles and were cast into 1-1/2" diameter water cooled copper molds. The larger 15 to 20 kg melts were made in Magnorite (Norton commercial MgO) crucibles of lower purity than the small crucibles. These larger heats were poured into either 3" diameter water cooled copper molds or into 3" diameter graphite molds. The summary of melts appears in Tables I, II, III, and IV.

The solution of niobium in uranium is a function of temperature, time, and agitation in the melt. Once the niobium is in solution there is no appreciable segregation in the ingot. In the 15 - 20 kg melts in the Magnorite crucibles it was necessary to go to 1500°C to dissolve all of the niobium. When melts were made at lower temperatures, pieces of niobium cubes could be seen in the crucible skull after pouring. In ingot L-8 where only 1400°C was reached, less than half of the niobium went into solution. In making the 5 kg melts of the 1-1/2% Nb + 5% Zr in the high purity magnesia crucibles, the initial practice was to take the melt to 1550° to 1650°C for a few minutes to insure the solution of niobium. After analysis became available, melt H-324 was made by holding for one hour at 1400°C to 1425°C and all of the niobium went into solution. In these 5 kg melts made in high purity magnesia crucibles, there was considerable agitation of the melts due to the magnesium boiling off. This probably helped in dissolving the niobium. In the larger melts made in the Magnorite crucibles there was also some magnesium boiling, but to a much lesser degree.

The zirconium appears to segregate at the top center of the ingots when analysis was taken from a small area just below the primary shrink pipe. It is thought that this additional zirconium is present as zirconium carbides and/or zirconium nitrides that are rejected to the top center of the ingot on freezing. It is also possible that they are pieces of the thin skull which floats on the melt in the crucible and which fall into the mold at the end of the pour and are trapped near the top center of the ingot during solidification.

TABLE I

5 Kg Melts of 1-1/2 w/o Nb + 5 w/o Zr Made in High Purity Magnesia Crucibles and Cast into Water Cooled Copper Molds

Casting No.	Location of Sample	w/o Nb	w/o Zr	C (ppm)	N (ppm)	B (ppm)	Melt Temp. Max. °C	Melt Temp. Pouring, °C
N-316	Top	1.55	5.52	26,26	21,23	0.2	1600	1450
	Bottom	1.55	5.38	19,22	10,19	0.4		
N-317	Top	1.57	5.40	*68,63	51,42	0.4	1650	1380
	Bottom	1.60	5.36	23,24	30,21	0.2		
N-318	Top	1.57	5.26	22	41,21	0.2	1600	1380
	Bottom	1.50	5.08	19	43,49	0.2		
N-319	Top	1.62	4.9	63,62	86,56	0.2	1630	1350
	Bottom	1.42	5.88	42	93,96	0.2		
N-320	Top	1.52	5.38	16	25,28	0.4	1600	1375
	Bottom	1.54	5.39	7	10,15	0.4		
N-321	Top	1.56	5.42	17	54,59	0.2	1600	1500
	Bottom	1.61	5.49	14	43,47	0.2		
N-322	Top	1.61	5.61	16	37,30	0.6	1550	1400
	Bottom	1.57	5.31	13	50,30	0.2		
N-323	Top	1.61	5.29	5	< 10,17	0.4	1500	1350
	Bottom	1.60	5.41	9	15,<10	0.4		
N-324	Top	1.63	5.33	21	66,80	0.5	1425	1400
	Bottom	1.60	5.16	25	100,90	0.5		
N-325	Top	1.52	4.95	14	53,39	0.1	1550	1450
	Bottom	4.98	4.98	13	28,38	< 0.1		

TABLE II

15 to 20 Kg Melts of 1-1/2 w/o Nb + 5 w/o Zr Made in Magnorite Crucibles and Cast into 3" Diameter Water Cooled Molds

Casting No.	Location of Sample	w/o Nb	w/o Zr	C (ppm)	N (ppm)	B (ppm)	Melt Temp. Max. °C	Melt Temp. Pouring, °C
L-6	Top Center	0.65	5.17	60,70	38	---	1400	1400
	Top Outside	0.63	4.83	50,70	19	---		
	Bottom	0.63	4.81	37,43	18			
L-19*	Top Center	0.68	5.19	20,20	10	---	1400	1400
	Top Outside	0.66	4.49	10,16	10			
	Bottom	0.64	4.70	11,14	10			
L-24**	Top Center	1.63	5.42	60	102	2	1500	1400
	Top Outside	1.56	5.09	33	31			
	Bottom	1.57	5.29	23	85			

*Remelt of L-6 except for skull.

**Remelt of L-23 which was heated to 1400°C and could not be poured because of a broken stopper rod.

TABLE III

Uranium-Zirconium Alloys: Melted in High Purity MgO Crucibles; Cast into 1-1/2" Diameter Water Cooled Copper Molds

Casting No.	Location of Sample	w/o Zr	C (ppm)	N (ppm)	B (ppm)	Melt Temp. Max. °C	Melt Temp. Pouring, °C	Depth of Primary Pipe (in.)
H-314	Top Center	1.46	45	505,515		1425	1300	1-1/4
Nominal	Top Outside	1.10	8	70,105				
1.0% Zr	Bottom	1.09	11	60,50	< 0.1			
H-315	Top Center	1.77	24	300,290		1375	1300	1
Nominal	Top Outside	1.54	8	53,57				
1.6% Zr	Bottom	1.55	7	55,53	< 0.1			
H-326	Top Center	1.95	6	23,34		1500	1400	2-1/4
Nominal	Top Outside	1.93	11	34,21				
2.0% Zr	Bottom	1.84	7,5	62,34	0.2			
H-327	Top Center	3.93	12	24		1525	1375	1
Nominal	Top Outside	3.89	19	---				
4.0% Zr	Bottom	3.93	6	19	0.3			
H-328*	Top Center	9.09	23,28	34	0.5	1625	1500	3/4
Nominal	Top Outside	8.28	8	43	0.3			
9% Zr	Bottom	8.26	10	35	0.3			

*One kg melt poured into 1-3/8" diameter water cooled mold.

Note: Top Samples were taken just below the primary pipe.

TABLE IV

15 to 20 Kg Melts of 3 w/o Niobium Alloys: Melted in Magnorite Crucibles; Cast into 3" Diameter Heated Graphite Molds

Casting No.	Location of Sample	w/o Nb	C (ppm)	N (ppm)	B (ppm)	Melt Temp. Max. °C	Melt Temp. Pouring, °C
L-36*	Top Center	3.47	170,160	95,93		1400	1400
(3rd melting)	Top Outside	3.28	140,135	84,80	12		
L-37	Top Center	3.35	170,170	66,68	2	1550	1400
(4th melting)	Top Outside	3.25	160,165	52,70	12		

*Previous melt was up to 1500°C and metal leaked from crucible.

Crucible life of the high purity magnesia crucibles has been very poor when making the 1-1/2% Nb + 5% Zr alloys. Every crucible was cracked or cracked shortly after it was removed from the furnace. The skull from these alloys is very adherent and appears to have considerable strength. This strong skull, along with its lower coefficient of expansion than magnesia, was the probable cause of the numerous cracks in each crucible. This alloy also attacked the magnesia crucible during melting and caused considerable evolution of magnesium vapor so that the melt was continually boiling. While this probably aided in the solution of the niobium, it caused the sight glasses to darken so rapidly that it was difficult to get accurate optical temperature readings. These crucibles had a life of 2 - 3 melts when making the straight zirconium alloys at lower temperatures. However, there was still considerable evolution of magnesium and darkening of sight glasses.

The crucible life of the Magnorite crucibles was only 1 to 2 melts. Failure started with cracks radiating from the drilled pouring hole, and spread from the outside bottom of the crucible up into the inside bottom. This caused several melts to leak through crucibles.

The internal quality of the 3" diameter water cooled ingots was poor. Longitudinal sectioning of several ingots revealed secondary pipe and shrink which persisted down the central portion of the ingot to within 1-1/2" of the bottom. The use of water cooled molds for 3" diameter ingots has been discontinued during this quarter, and all subsequent castings of 3" diameter ingots are made in heated graphite molds.

There are not sufficient data available to draw any conclusions on the effects of segregation, but it is certain that the internal quality of metal cast into heated graphite molds is far superior to that cast into water cooled copper molds.

The internal quality of the 1-1/2" diameter ingots cast into water cooled copper molds is somewhat better than that of those cast into 3" diameter water molds. However, secondary pipe, shrink holes, and bright, smooth gas pockets have been found in ingots cast into 1-1/2" diameter water cooled molds. It is felt that the rapid pouring of these 1-1/2" diameter ingots causes an excessively deep molten pool which bridges over by side cooling. It is hoped to improve this condition by going to a smaller pouring hole than the 1/2" diameter one now being used.

There is a new type of defect which has been appearing in a majority of the castings made in the 1-1/2" diameter water cooled copper molds during this quarter. It is a blowout or boiled out appearance at the top of the ingot. It is a shell about 1/8" to 3/16" thick, and 1" to 2" high, that stands on top of the ingot and appears to be quite porous. It is speculated that the ingot boiled up in the mold just after it was poured and that this shell was formed

by freezing of boiling metal. These ingots have about the same internal and external quality after this top shell and the primary pipe have been cut off as ingots which do not exhibit this type of shell at the top. This defect appears erratically, and the present work to eliminate it is concentrated along the lines of more thorough cleaning of raw materials. It is felt that some heavy hydrocarbons remaining from cutting coolant are not completely cleaned from the biscuit. It is speculated that these distill off from the metal during the heating process and condense on the cold mold. This condensate then is revaporized as metal is poured into the mold, causing the metal to boil.

The pickup of carbon and nitrogen in the melts continues to follow erratic patterns. Generally speaking, remelting lowers carbon and nitrogen. Occasionally it does not help, and it is thought that these ingots were not thoroughly cleaned of cutting oils and compounds when they were prepared for remelting.

2. Development of High Temperature Strength Zirconium and Titanium Base Alloys (K. F. Smith, H. H. Chiswik)

Corrosion and thermal conductivity tests have been made on some zirconium base and titanium base alloys as preliminary screening criteria for their suitability as jacketing materials of high temperature strength.

Zirconium Alloys in Static Degassed Water at 360°C

Zr-4% Al, 45 hours	Very poor
Zr-7% Ti, 45 hours	Fair; greyish coating over black oxide
Zr-7% Ti, 1 week	Very poor

Titanium-8% Al in Static, Air-Saturated Water

Very good. The table below shows data obtained in successive runs with the same two specimens.

Time of Exposure	Temperature (°C)	Weight Change (mg/cm^2-month)
186 hours	93	+1.22
330 hours	260	-0.61
712 hours	260	+0.124
1 month	260	-0.02
2 months	260	-0.06
2 weeks	360	+0.263
1 month	360	0.000
2 months	360	+0.047
1 month	360	0.000

The thermal conductivities of these alloys were as follows:

Nominal Composition	Mean Test Temperature (°C)	Thermal Conductivity ($cal/cm^2/sec/°C/cm$)
Zr-4% Al	45.5	0.020 (4.9)*
Zr-7% Ti	46.5	0.031 (7.4)*
Ti-8% Al	44.2	0.022 (5.4)*

*$BTU/hr/ft^2/°F/ft$

IV. BASIC METALLURGY

1. Self-Diffusion in Uranium (R. Weil, S. H. Paine)

An effort is in progress to make a direct determination of the self-diffusion coefficient of uranium by using U^{235} as a tracer isotope. The method we have selected as most promising for achieving the necessary interface between isotopes is vapor deposition by cathodic sputtering in purified argon at low pressures.

Feasibility tests are now being made in a specially designed apparatus. Several successful deposits of uranium on copper and on uranium have been obtained at about 20 microns pressure. The uranium cathode is a thin-walled, hollow cylinder, 1-1/4" high and 1-7/8" inside diameter. A 1/8" diameter pin is located at its axis to receive the sputtered metal. Before sputtering, a copper cylinder is inserted between the uranium and the pin and is made anodic with reference to them. In this manner, any oxide remaining on the pin or the uranium cylinder is removed. The copper cylinder is then raised and the uranium is permitted to sputter onto the pin.

Figure 1 shows a cross section of layers of uranium approximately 0.5 and 2.0 microns thick sputtered on a copper pin. The rate of deposition was 0.03 micron per hour per ma of current. The process was intentionally interrupted for about a day to test the adhesion of one layer of uranium to the other. In actual practice, the deposition will be continuous.

2. Deformation of Alpha Uranium Single Crystals (L. T. Lloyd, H. H. Chiswik, M. D. Odie)

The compressive deformation characteristics of eleven additional single crystals of alpha uranium have been studied. The directions of compression of these crystals, with respect to one quadrant of a (001) standard projection, are shown in Figure 2. The majority of these orientations were chosen to further plumb out the deformation mechanisms resulting from compressive loading at room temperature. Most of the orientations studied were designed to exclude or minimize slip on the (010) plane in the [100] direction by choosing directions that were nearly 90 degrees to these elements. Two of the directions were chosen in attempts to verify previously reported deformation mechanisms: Crystal N was oriented most favorably for slip on a $(1\bar{1}0)$ plane in a [110] direction (slip system reported by Cahn)[5] and Crystal M was oriented such that maximum contraction of the crystal would result if irrational $\{176\}$ type twinning occurred (twin system reported in ANL-5036).

---

[5] R. W. Cahn, "Plastic Deformation of Alpha Uranium; Twinning and Slip," Acta Metallurgica, Vol. 1, No. 1, pp 49-70, January 1953.

Figure 1. Sputtered Uranium Layer on Copper.

Micro #15536 2100-X

Figure 2. Quadrant of a (001) Standard Projection Showing the Crystallographic Locations of the Directions of Compression of the Eleven Crystals Studied.

Macro #15524

Cahn has reported, in addition to slip on the (010) plane in the [100] direction, a second slip system involving {110} planes and <110> directions. In our studies to date, no positive identification of the latter slip mechanism has been obtained. In order to test its existence, a crystal was oriented such that compression would result in a maximum shear stress on a {110} plane and in a <110> direction. Because of the orthorhombic crystal structure of alpha uranium, there are two directions that would be inclined 45 degrees to a {110} plane and a <110> direction. The direction of compression of Crystal I, reported in ANL-5234, very closely approximates one of these directions (3 degrees from the ideal direction), but no {110} - <110> slip was observed. The second compression direction is 19 degrees from the [100], 71 degrees from the [010] and 90 degrees from the [001]. Crystal N was prepared for compression in this direction. Three compressive tests performed on this crystal resulted in deformation by (010) plane slip only, even though it was relatively unfavorably oriented for deformation by this mechanism. The results obtained on Crystal N coupled with those for Crystal I indicate that slip on a {110} plane and in a <110> direction does not occur in alpha uranium when deformed at room temperature.

Four of the crystals studied (L, S, U and P) have orientations which lie close to the zone of poles connecting the (001) and (010) poles. The directions of compression of these are all close to 90 degrees from the [100] direction and therefore should suppress deformation by (010) plane - [100] direction slip. All of these crystals showed deformation by the two {130} type twins. Crystals U and P also exhibited deformation by two of the four irrational {172} type twins. Also, all of these crystals showed (010) plane slip traces. This slip is believed to be the result of {130} twinning accommodation within the parent crystal. The slip traces observed were always in the vicinity of {130} twins and especially near localities of impingement of the two twins of this system.

The orientation of Crystal V was chosen with no specific deformation mechanism in mind, but generally to test for the operative deformation mechanisms in this region of the standard projection. Three deformation mechanisms were found: slip on the (010) plane in the [100] direction; twinning on one of the four irrational {172} planes; and twinning on one of the two {130} planes.

Crystal M was oriented for compression in a direction for which the formation of irrational {176} type twins would result in a maximum contraction. Notwithstanding this, compression in this direction failed to yield the {176} type twins, and deformation occurred primarily by slip on the (010) plane. In addition to the (010) slip, an irregular deformation trace was observed on one of the metallographic faces. The nature of this irregular type trace is discussed below in connection with its appearance in some of the other crystals where it could be analyzed in better detail.

Crystals O, T, R, and Q were compressed in directions nearly 90 degrees from the (010) plane. These orientations should also minimize deformation by slip on the (010) plane in the [100] direction; yet, in all cases this mechanism was not completely suppressed. Crystals O and T deformed primarily by kinking. In addition to this kinking, Crystal O also deformed generally by (010) slip, and Crystal T exhibited irregular deformation traces similar to those observed on Crystal M. Crystal R deformed primarily by (010) slip, and also showed irregular deformation traces similar to those observed on Crystals M and T.

Crystal Q resulted in a good example of the type of deformation involving the "irregular" traces. Low magnification observations of this crystal after the first compression showed a general roughening of the two metallographic faces and the presence of distinct irregular traces near the bottom compression face. At high magnification, each of the two faces showed two slip trace directions (Figure 3). One of these directions, on each face, appeared almost parallel to the common edge, was quite distinct, and was readily located with respect to the common edge. One-surface analysis indicated these two traces to have their origin in (010) plane slip. The other two traces were more difficult to locate with respect to the common edge. It was, however, possible to take angular measurements of the trace directions which agreed reasonably well. Two-surface analysis (Figure 4) of these indicated that the (001) plane was the plane of slip. This was substantiated further by the following observations: The sides of the crystal were close to being (010) planes and contained rather distinct slip markings. Since one of the systems was identified as (010) plane slip, these traces could not be the result of that system of slip. One-surface analysis of the markings indicated that their loci of poles passed close to the pole of the (001) plane.

Figure 3 shows a photograph of face A in the region of the distinct irregular traces. The appearance of the slip traces is typical of that resulting from cross slip. Cahn reported the occurrence of cross slip in connection with (010) plane slip, but made no identification of the second slip plane. The present results indicate this plane to be the (001). If this is true cross slip, the slip direction for the (001) slip should be the same as that for the (010) slip, namely the [100] direction. There is some circumstantial evidence that this is so, from the fact that the gross displacement of one end of the crystal with respect to the other as a result of these irregular traces, especially as observed after the second compression, was in the general direction of the [100]. In addition, there was some asterism of Laue spots which would indicate a rotation of the lattice about the [010] direction. This is the type of asterism that one would expect from slip on the (001) plane in the [100] direction. It must, however, be pointed out that it was impossible to precisely solve for the rotation about the (010) pole because of the asterism of the spots resulting from the accompanying slip on the (010) plane in the [100] direction.

Figure 3. Photograph Taken from Face A of Crystal Q After First Compression in Region Near Distinct Markings.

The right hand edge of the photograph corresponds to the common edge of the crystal. Note the faint irregular traces observed throughout the photograph and the distinct marking resulting from slip on the (010) and (001) planes. The area best illustrating the existence of cross slip appears in the lower center portion of the photograph.

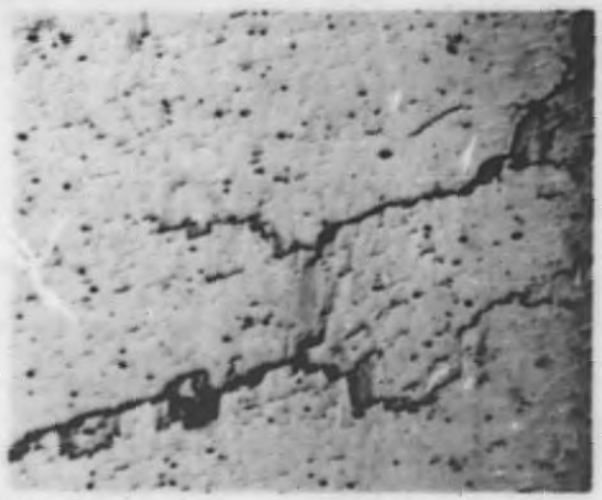

Micro #15294 Bright Field 250-X

Figure 4. Stereographic Projection on Face A of Crystal Q Showing Two-Surface Analysis of (001) Cross Slip Traces Observed After Compression.

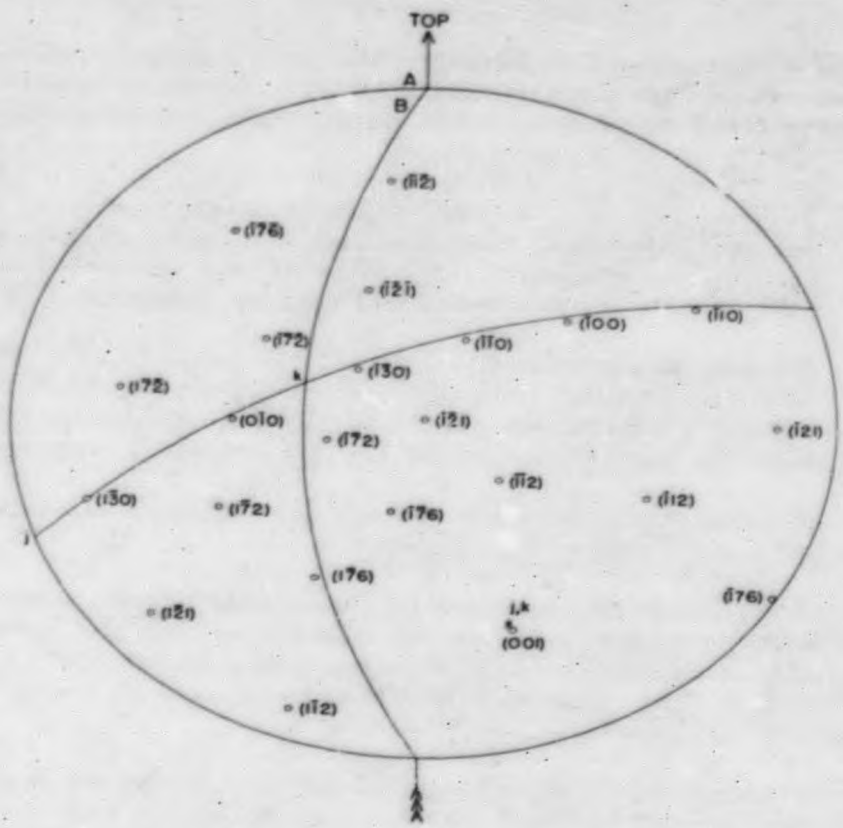

Macro #15312

Additional evidence that the minor slip traces originate from (001) planes was found in the other three crystals (M, R and T) that exhibited this type of deformation. One-surface analysis for all of these crystals showed that the secondary slip trace directions had loci of poles that pass near the (001) plane pole. A higher magnification photograph (Figure 5) taken from Crystal T after the fourth compression showed the same type of cross slip traces observed on Crystal Q.

3. The Constitution of the Uranium-Carbon Alloys (B. Blumenthal, B. G. Allen)

Alloy Preparation: Because of the need for uranium-carbon alloys of more uniform carbon distribution than were obtained heretofore, the method of preparing these alloys was modified to comprise the following steps:

1. Preparation of a uranium-carbon master alloy by melting high purity electrolytic uranium crystals in a graphite crucible for 15 minutes at 1400°C. No attempt was made to attain equilibrium or to obtain a predetermined carbon content.

2. Melting of variable portions of this master alloy together with more electrolytic crystals in a urania crucible for one hour at 1400°C. This temperature is high enough above the anticipated liquidus temperatures for the total carbon to go into solution.

3. Transporting the melt quickly into the cold end of the furnace tube for rapid solidification.

Three ingots were prepared by this method in a vacuum resistance furnace. Their composition at the top, the center and the bottom are shown in Table V. No contamination by other elements above that of high purity metal occurred in these ingots except for nitrogen; a few areas of high nitrogen concentrations were found.

Metallography of Uranium-Carbon Alloys: The first series of uranium-carbon alloys having a carbon content of 250 and 500 ppm were metallographically examined after annealing at 700° to 1100°C in increments of 100°C. First the entire ingots were homogenized at 1000°C for five hours. Specimens of 5 to 10 grams weight were cut from these ingots, carefully wrapped in tantalum foil, sealed in Vycor tubes (the 1100°C series in a quartz tube) at vacua of 4×10^{-7} to 2×10^{-6} mm Hg and suspended on a thin wire in a vertical tube furnace for these periods of time:

at 700°C for 3 days
at 800°C for 24 hours
at 900°C for 5 hours
at 1000°C for 3 hours
at 1100°C for 1 hour

Figure 5. Irregular Traces and Cross Slip Observed on Crystal T. After Fourth Compression.

The vertical slip lines are caused by (010) plane slip. The irregular traces are the result of (010) and (001) cross slip.

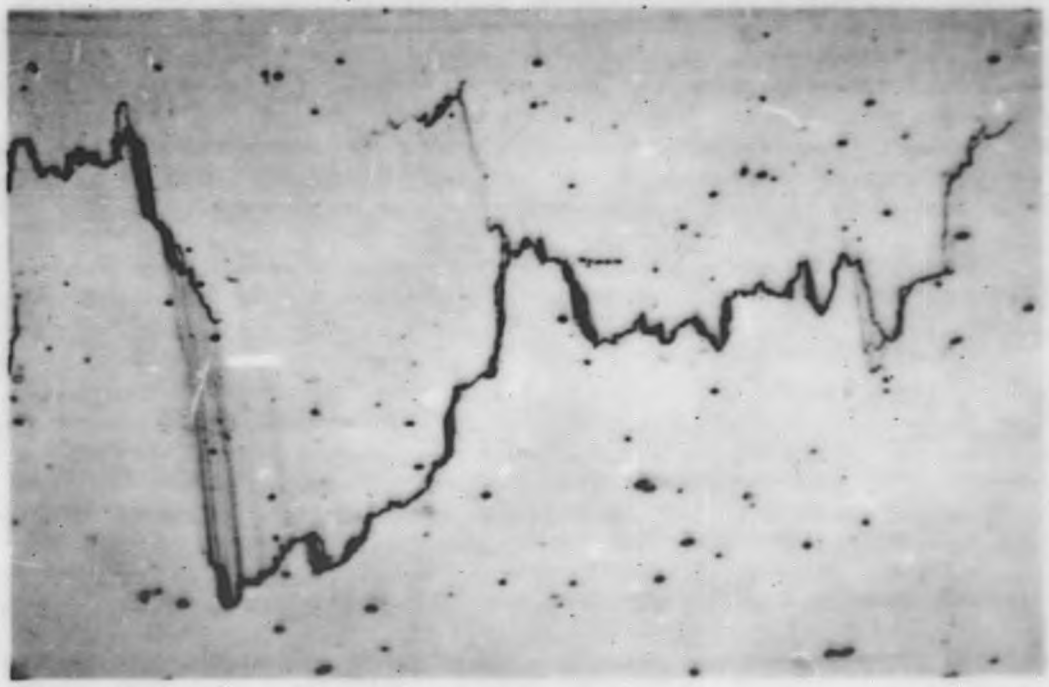

Micro #15496 Bright Field 500-X

When the anneals were completed, the suspension wire was cut and the sealed tubes dropped into a bucket of water. The tubes were broken by an electromechanical device. This device consisted of a small lever that closed a microswitch when the falling sealed tube hit it at the bottom of the water bucket. The microswitch operated a solenoid which provided the power for a hammer-like arm to hit the sealed tube and break it. A second solenoid withdrew the arm after the blow so that the water would have unhindered access to the specimens. The device included a guide tube and was mounted on a horizontal plate resting on the rim of the bucket of water. Quenching by this device was better controlled than was possible by the normal method of hitting the sealed tube with a hammer after it has been dropped into the water.

Micrographs of this series of experiments are shown in Figures 6 through 8. Figure 6 shows the microstructure of an alloy of 500 ppm carbon after annealing at 700°C and water quenching. The three days anneal did not suffice to form distinct precipitated particles; however, the Widmanstatten patterns of binary grains indicate that the rejection of the solute from its matrix had commenced. How much of this phenomenon was caused by the change in solid solubility due to the gamma-beta transformation and how much of it was perhaps due to the beta-alpha transformation cannot be stated at this time Anneals of longer duration are in process.

At 800°C an alloy with 250 ppm carbon showed carbide precipitation in the form of a very fine network. Figure 7-a is typical of the structure near the center of the specimen. The amount of precipitate increases as one moves from the center towards the periphery (Figure 7-b) contrary to expectations if one assumes the quench to be more effective at the outside than at the center of the specimen. It has previously been observed that well quenched specimens form alpha grain of markedly irregular shape. The present series does not conform to this observation. It is possible that the technique of quenching several specimens simultaneously may have caused this effect and that the present series does not necessarily reflect the structure of the specimens at their heat treating temperature. Less precipitate is observed in the center of the 900°C annealed alloy (Figure 7-c), again with the amount of precipitate increasing towards the edge (Figure 7-d). At 1000°C very much precipitate is found at the edge (Figure 7-f). Its irregular distribution extends to the center (Figure 7-e) which also shows fine particles along the grain and subgrain boundaries at the alpha phase. At 1100°C much of a second phase is found throughout the specimen, apparently in uniform distribution (Figure 7-g), at a carbon content of about 250 ppm. This same second phase can be more readily resolved in alloys containing 500 ppm carbon, and at high magnification reappears as a constituent of the same color as the primary angular carbide inclusions (Figures 8-a and -b).

Figure 6. Uranium-Carbon Alloy (B465) [500 ppm Carbon].

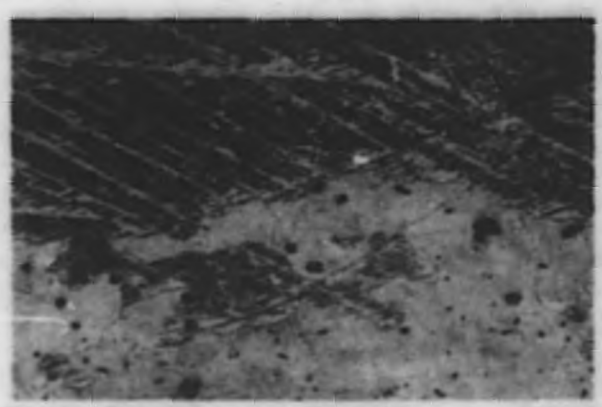

Micro #15257 Etched 100-X

Water Quenched from 700°C.

Figure 7. Uranium-Carbon Alloy (B459) [250 ppm Carbon].

7-a. Water Quenched from 800°C.

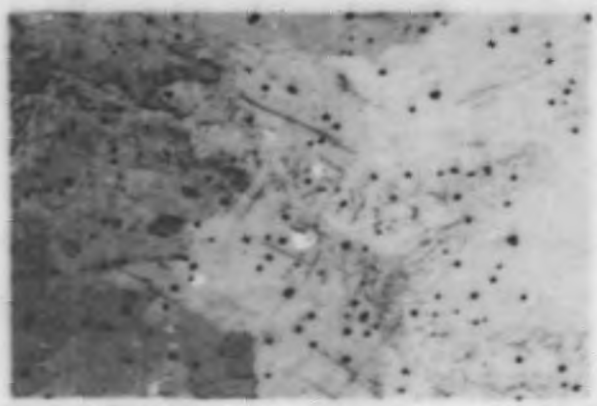

Micro #15277 Etched 100-X

Center of Specimen.

7-b. Water Quenched from 800°C.

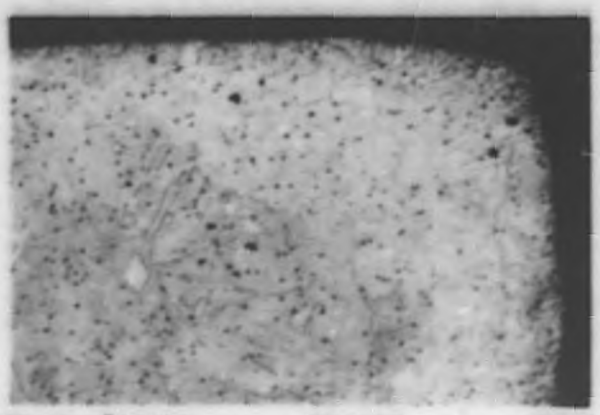

Micro #15551 Etched 50-X

Corner of Specimen.

7-c. Water Quenched from 900°C.

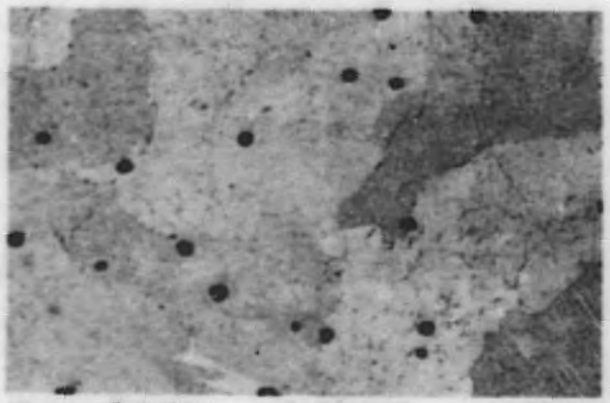

Micro #15040 Etched 100-X

Center of Specimen.

7-d. Water Quenched from 900°C.

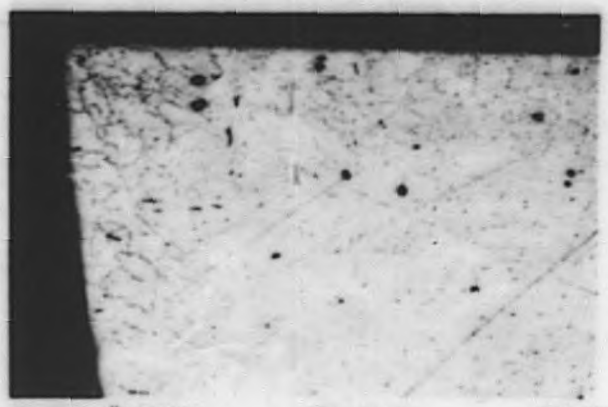

Micro #15553 Etched 50-X

Corner of Specimen.

7-e. Water Quenched from 1000°C.

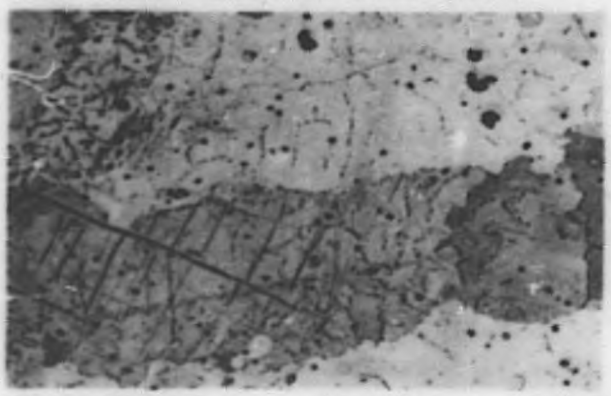

Micro #15352 Etched 100-X

Center of Specimen.

7-f. Water Quenched from 1000°C.

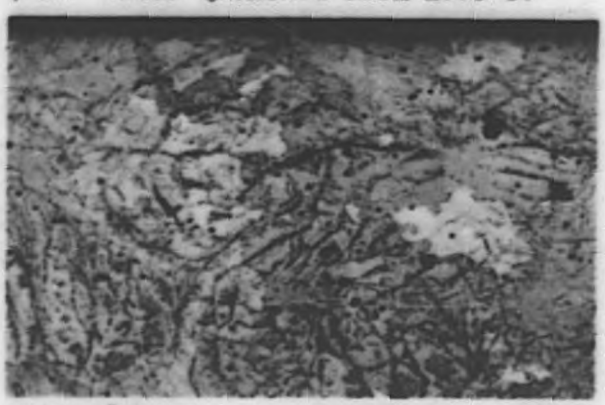

Micro #15351 Etched 100-X

Edge of Specimen.

7-g. Water Quenched from 1100°C.

Micro #15355 Etched 100-X
Center of Specimen.

Figure 8. Uranium-Carbon Alloy (B461) [500 ppm Carbon].

8-a. Water Quenched from 1100°C.

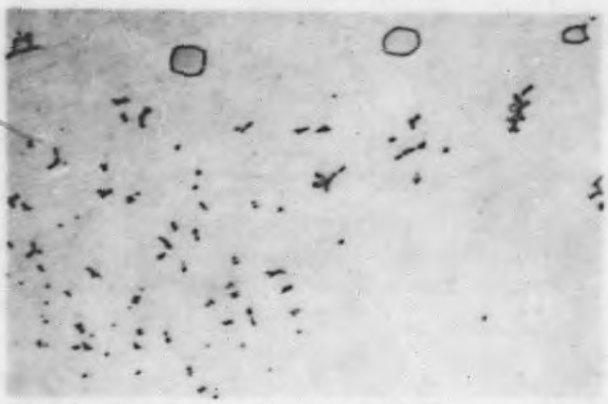

Micro #15349 As Polished 500-X

8-b. Water Quenched from 1100°C.

Micro #15350 As Polished 2000-X

No attempt is made at this time to interpret these micrographs relative to the constitution of the uranium-carbon alloys. It appears that, at least at higher temperatures, the problem of contamination of the specimens from the Vycor or quartz tubes is not yet solved. A furnace for annealing in a highly purified helium atmosphere is being built. This furnace should eliminate the suspected contamination and also provide for a better quench than is possible by the present sealing and fracturing method.

TABLE V

Composition of High Purity Uranium-Carbon Alloys

Melt No.	Sample Location	Carbon in ppm		Nitrogen (ppm)
		ANL Data	Average	
B492	Top	130, 140, 100		18
	Center	110, 103	113	<10
	Bottom	106, 102, 115		44
B493	Top	200, 200		22
	Center	215, 222	204	11
	Bottom	205, 180		11
B497	Top	257, 253		54
	Center	245, 230	259	11
	Bottom	280, 289		13

4. The Constitution of Uranium-Zirconium Alloys (S. T. Zegler, H. H. Chiswik, M. H. Mueller, S. Hayes)

Heat Treatment and Microstructure: The series of uranium-zirconium alloys (0.09 to 2.5 w/o Zr) discussed in ANL-5234 have been heat treated isothermally at 400°C and 500°C for periods varying from 5 seconds to 5 minutes, followed by water quenching. Specimens were in the form of discs, 1/2" in diameter ("as rolled" size) by 0.050" thick; solution treatment was done in salt at 800°C for 2 minutes. The microstructural observations may be summarized as follows: (1) No differences exists in the microstructures of specimens held for 5 seconds and 5 minutes at 400° or 500°C, suggesting that transformation probably occurs in less than 5 seconds at either of these temperatures; (2) The microstructures do not differ from those obtained on direct quenching from the gamma temperatures. Up to about 1 w/o Zr, the structures consist of typical large grained alpha uranium; at the higher zirconium compositions (1.6 w/o and 2.3 w/o), a heterogeneous acicular structure is obtained which shows evidences of beginning of decomposition on holding at 400° - 500°C for 5 minutes, as illustrated in Figure 9.

Considerable peripheral inclusion segregation was noted in the specimens with zirconium contents above 0.21 w/o, as shown in Figure 10. This segregation cannot be ascribed to the heat treatments, since it was present in the "as rolled" rods, and is probably related to mold side-wall segregations in the castings. The extent of this segregation is illustrated in Figures 11-a and -b for the interior and periphery, respectively.

Nature of Epsilon Phase: Debye X-ray diffraction patters were obtained on alloys containing 10 w/o, 30 w/o and 53 w/o zirconium after various heat treatments. The alloys were prepared by arc melting zirconium crystal bar and normal uranium plate. The nominal 53 w/o Zr-U analyzed 51.9 w/o Zr, 142 ppm nitrogen, and 100 - 175 ppm carbon. After casting, the alloys were hot swaged at 800°C to promote homogeneity, and water quenched after the last swaging operation. Slivers, 1/16" square x 3/4" long, were cut and heat treated as described below for X-ray analysis. The slivers were cleared of oxide by grinding on metallographic papers under water through #400 grit and pointed to less than 0.001" at one end with #600 grit paper in a pin vise in a drill press. They were then electropolished for 1-1/2 to 3 seconds in acetic-perchloric acid solution[6] at 80 volts (1 amp). Polishing resulted in very bright surfaces which were unattainable using the phosphoric acid solution generally applicable to unalloyed uranium. The slivers were heat treated wrapped in tantalum sheet in a vacuum (10^{-4} mm Hg) in Vycor tubing. After heat treating, the slivers were again electropolished. X-ray diffraction patterns were taken using a 114.6 mm diameter camera and filtered Cu Kα radiation. In the case of the 53 w/o Zr-U alloy, X-ray diffraction patterns

[6] 100 cc perchloric acid
2000 cc acetic acid (glacial)

Figure 9. Typical Microstructure of Alloys Containing 1.6 and 2.3 w/o Zirconium After Isothermal Treatment at 400°C or 500°C.

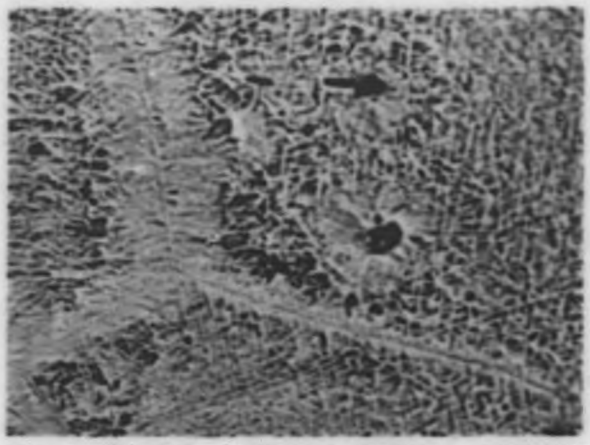

Micro #15101 Bright Field 1350-X
Ames Etch

Figure 10. Peripheral Inclusion Segregation.

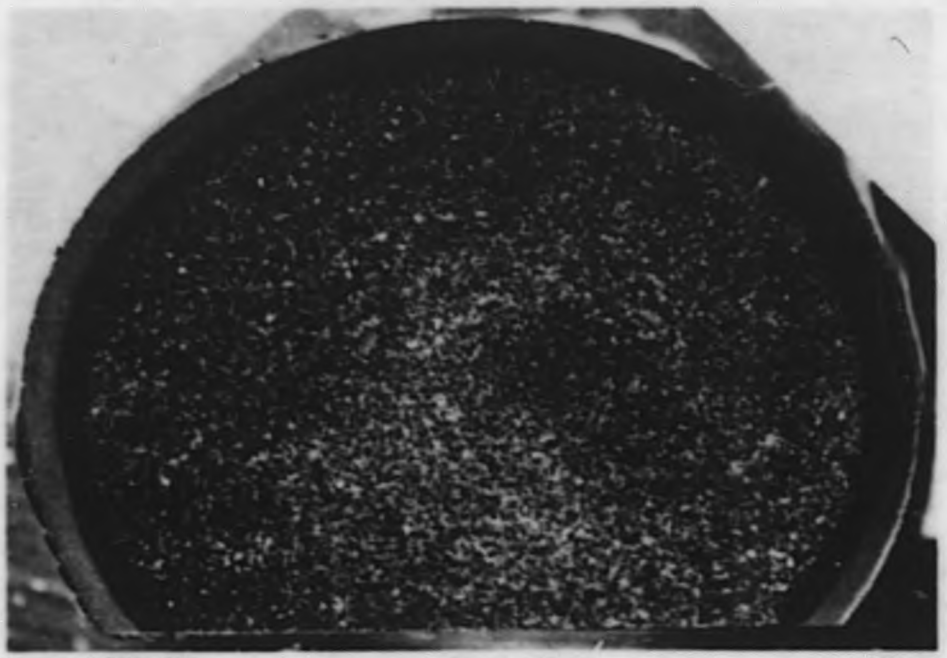

Macro #15102 Ames Etch 10-X

Figure 11. Extent of Inclusion Segregation in Interior and Periphery.

11-a. Interior.

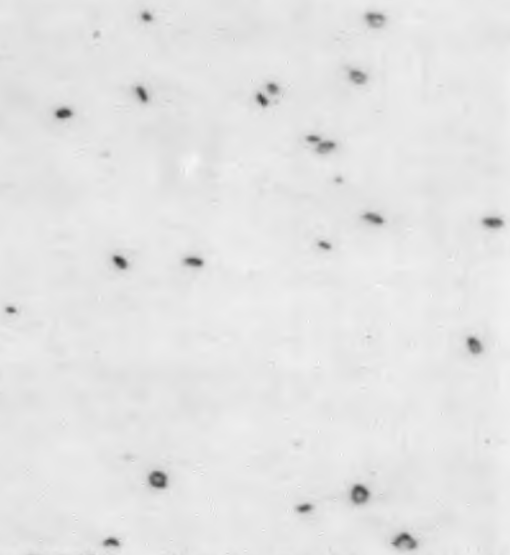

Micro #15083 Bright Field 2000-X
H_3PO_4

11-b. Periphery.

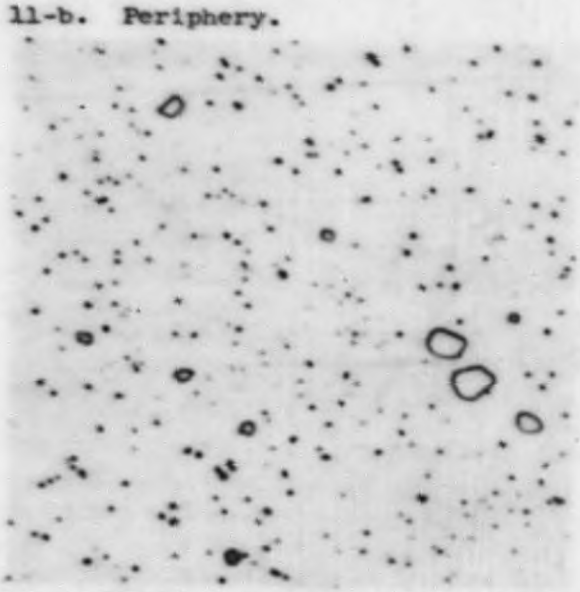

Micro #15084 Bright Field 2000-X
H_3PO_4

were also taken at elevated temperatures. The samples for the high temperature pictures consisted of a sliver similar to the ones described above. A vacuum of 10^{-5} to 10^{-4} mm Hg was maintained in the camera during the heating, which was sufficient to prevent the oxidation of the sample surface, even after a number of exposures.

The heat treatments included the following:

a. 2 hours and 1 week at 1000°C and water quenched.
b. Gamma quenched as above and annealed for 1 week at 560°C and water quenched.
c. Gamma quenched, cold worked, annealed 24 hours at 590°C and water quenched.

High temperature patterns were taken at 450°, 500°, 600°, 610°, 682°, and 725°C.

Quantitative evaluation of the patterns has not yet been made. Qualitatively, however, the following tentative observations may be noted.

1. Some specimens of the 53 w/o Zr alloy quenched from the gamma phase yielded a body centered cubic pattern only, which could be interpreted as retained gamma, other specimens, however, yielded the same body centered cubic lines plus "extra" lines which could not be ascribed to either alpha uranium or alpha zirconium. The reason for this discrepancy is not clear. Microscopic examination of this alloy (not the X-ray specimen) indicated a single phase (see Figure 12), suggesting the possibility that the body centered cubic lines arise from the same phase, causing the "extra" lines.

2. Specimens of the 53 w/o Zr alloy quenched from the gamma, cold worked, and annealed at 590°C and water quenched yielded alpha uranium lines, alpha zirconium lines along with the "extra" lines pattern present in the "as quenched" condition (which include the body centered cubic lines).

3. Patterns obtained at temperatures of 680° and 725°C could be identified as the alpha zirconium and body centered cubic gamma solid solution, as would be expected from the equilibrium diagram.

4. A pattern obtained at a temperature of 610°C consisted of alpha uranium and alpha zirconium only. This result is not in agreement with the presently available phase diagram.

5 Patterns obtained at temperatures of 450°, 500°, and 600°C, all contained alpha zirconium and alpha uranium lines, or alpha zirconium lines only, plus the "extra" line pattern.

Figure 12. Uranium-53 w/o Zirconium Alloy Heat Treated One Week at 1000°C; Water Quenched. Etched in Acetic-Perchloric Solution.

12-a. At 50-X Magnification.

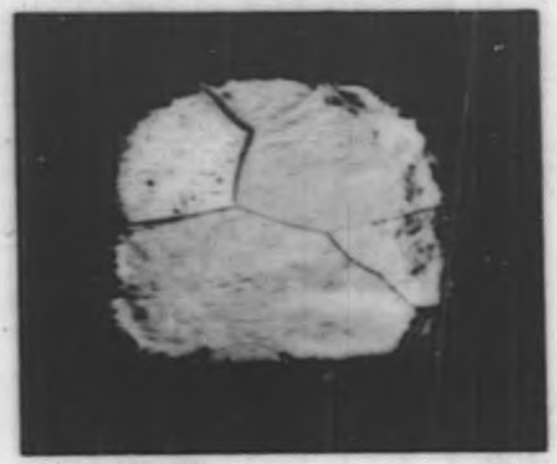

Micro #15548 50-X

12-b. At 250-X Magnification.

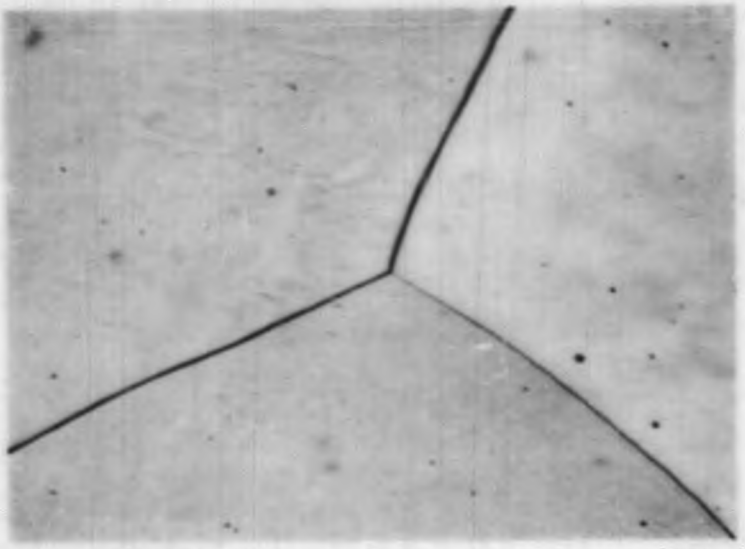

Micro #15547 250-X

6. The "extra" lines pattern apparently constitutes the epsilon phase and was present in the gamma quenched 10 and 30 w/o Zr alloys.

7. From the results of patterns taken at temperature, it would appear that the epsilon pattern can be formed from alpha uranium and alpha zirconium. Whether or not it can also be a direct decomposition phase from the gamma solid solution is not certain.

V. APPLIED METALLURGY

1. Zone Melting of Uranium Alloys (R. J. Dunworth, R. E. Macherey)

The zone melting of uranium rods described in the previous Quarterly Report, ANL-5234, has been continued. Since the early estimates of the speed at which the molten zone should move through the bar were greatly in error, the main emphasis has been to find the proper speed for obtaining the most effective "k" values. The ratio of the solute concentration at the solidus to the solute concentration at the liquidus is "k." The effective "k" is the apparent ratio actually obtained in a certain experiment. The data of the last melts indicate that, within a factor of 2 or 3, a speed of 1" per hour is suitable for carbon movement and 1/4" per hour is suitable for movement of the metallic solutes, such as iron, chromium, nickel, etc. The uncertainty in these values results from the following factors that make the effective "k" less efficient than the theoretical "k" which may be calculated from the phase diagrams: (1) the diffusion rates of the solute in molten uranium and solid uranium; (2) the degree of the thermal and magnetic stirring; (3) the irregularity of the solidifying interface; (4) the length of the molten zone; (5) the speed of the molten zone; and (6) phase diagram uncertainties.

At constant power input, the zone length varies from 3/4" in the center of the bar to 1-1/2" or 2" at both ends. The transfer of heat from the molten zone through the uranium rod is considered responsible for this variation. A number of resistors are being installed in the field circuit of the motor generator to correct this difficulty. Line voltage fluctuations, which also markedly affect the length of the molten zone, are being corrected by means of an electronic voltage regulator in the field circuit. The data from which the estimated speeds were obtained were single passes. With more passes and a better regulation of zone length, a greater accuracy in the determination of the effective "k" can be expected.

The analyses are listed for six zone melts in Table VI. All the rods were 15" long and 0.625" in diameter, fabricated from the same billet, melted in an Al_2O_3 boat (Norton RA98), with no wash, in a vacuum of about 0.001 microns, and were given one pass at the speeds listed. It may be noted in ZM16, ZM17, ZM20, and ZM24 that the carbon separation is about the same. The fastest speed, 1" per hour, was chosen for carbon removal. The movement of boron, iron, and silicon in ZM16 and ZM17 is more complete than at faster speeds. Other data (not listed) for movement of zirconium and vanadium in 2" alloy rods also show improved solute transfer at the slower speed. The speed of 1/4" per hour was chosen on the basis of these data. The fact that the metallic solutes are present in low amounts with possibly greater difficulties in analysis makes the optimum speed determination less accurate. Castings are being made in which the solute concentration will be 500 ppm to circumvent this factor of error.

TABLE VI

Single Pass Zone Melted Uranium Rods

Melt	Speed[1]	Sample[2]	C	N	Al	B	Cr	Cu	Fe	Mg	Mn	Ni	Si
ZM16	1/4	0	155/170[3]	40/32	7	2	5	1	30	2	3	15	20
		1	117	36, 21	15	0.7	5	2	10	1	<1	10	20
		2	150	<10	15	1.5	5	2	20	1	<1	15	15
		15.5	165	15, 11	50	5	10	2	50	<1	<1	30	30
		16	240	<10	40	30	30	2	200	<1	<1	60	150
ZM17	1	0	170/175	32/30	10	3	10	2	30	5	3	20	30
		1	143	19, 26	15	2	7	10	15	2	1	15	20
		2	115	17, <10	15	2	7	3	20	1	1	15	20
		15.5	155	25, <10	20	7	10	3	50	1	<1	30	30
		16	230	15, <10	20	13	30	4	150	2	1	70	60
ZM18	2	0	190/185	30	10	1	5	4	30	2	2	15	10
		1	140	41	10	3	5	4	20	1	1	10	10
		2	180	30	10	3	5	4	20	2	1	10	10
ZM19	4	0	168/185	38	10	2	5	1/2	20/30	2/3	3	10/15	10/20
		1	160	37	10	3	5	1	20	2	2	10	15
		2	140	42	15	3	7	1	40	1	3	15	20
ZM20	1/2	0	175/180	26	10	2	2	2	35	5	3	10	15
		1	135, 130	13, 17	10	0.5	2	1	10	2	2	5	10
		2	95, 95, 85	30	15	0.5	1	2	10	3	2	5	15
(4) ZM24	1	0	170	21	10	4	5	3	30	5	3	10	30
		1	135	19	10	1	2	1	10	2	1	5	20

(1) Speed, one pass in inches per hour.

(2) "0." analysis in ppm before melting.
"1." start of first zone.
"2." start of second zone.
"15.5." middle of last zone.
"16." end of rod or last zone.

(3) 155/170 = 155 ppm carbon at lead end of rod, 170 ppm at trailing end of rod.

(4) Boat had a ThO_2 wash.

Rods were 15" long and 0.625" in diameter, fabricated from the same billet, and were melted in a vacuum in an Al_2O_3 boat with no wash, except ZM24.

From phase diagram calculations, aluminum and silicon have a "k" of 0.3; chromium, iron and manganese, 0.1; copper, nickel and lead, 0.01. The good movement of chromium, iron and nickel substantiates these values. The values for aluminum, boron, and silicon are probably high due to contamination from the alundum boat which contains 10% SiO_2. A MgO wash used in earlier melts prevented aluminum contamination but the wash was attacked by the uranium. A ThO_2 wash was used on the boat for ZM24. The aluminum, boron and silicon contents are lower than in ZM17, which was made at the same speed in an unwashed boat.

In Table VII, the analyses for ZM9 and ZM10 are listed. These melts were made from the same high purity starting billet and were given 15 and 20 passes, respectively. The melting was done, however, at relatively fast speeds and the lack of theoretical separation is evident. MgO wash was used on the boats and no pickup of aluminum or silicon was obtained. Carbon in the first two zones of ZM10 amounts to 1/5 of the amount originally present. If the proper speed had been used, the carbon content should have been 0.2 ppm instead of 20 ppm. The value 0.2 ppm is estimated using an effective "k" of 0.5 and 15 passes. Boron, chromium, and iron were removed to below spectrographic limits. It may be noted that some nickel was found in the last zone when the feed bar analyzed <5 ppm. A method is indicated of concentration and finding elements initially present below analytical limits.

The zone melting process will certainly produce uranium metal of higher purity than presently available. It has a definite value in determining eutectic compositions and approximate limits of solid solubility at the eutetic temperature. For example, eutectic diagrams are formed by carbon, nitrogen and boron with uranium. The actual eutectic composition will be determined when a constant concentration is obtained over a definite length of the rod. The concentration will not change because the value of "k" becomes 1 at the eutectic composition. For this work, feed material concentrations near the eutectic value and/or both sides of the eutectic should be chosen. The eutectic composition for carbon in uranium is approximately 600 ppm, as determined by one zone melting experiment. The removal of fission products and concentration of plutonium would appear to be more promising if the speed zone travel could be increased. Some form of thermal, magnetic, mechanical or vibratory stirring in the molten zone might allow a faster speed. A direct current applied to the bar might increase solute movement in the molten zone. Certain experimental data are required for each application of zone melting before the process may be considered competitive.

TABLE VII .

Multiple Pass Zone Melted Uranium Rods

Melt	Speed	Sample	C	N	Al	B	Cr	Cu	Fe	Mg	Mn	Ni	Si
ZM9	15 (1)	0(2)	70/105(3)	13/<10	10	<0.1	1	1	5/10	1	<1	<5	10
		1	54	11	10	<0.1	1	1	8	1	<1	<5	10
		3	66	<10	8	<0.1	1	1	5	1	<1	<5	10
		5	77	<10	8	0.1	1	1	30	<1	<1	<5	10
		7	78	11	5	0.2	1	1	10	2	<1	<5	10
		9	90	<10	5	0.2	1	1	10	1	<1	<5	10
		11	125	<10	5	0.8	1	1	10	2	<1	<5	10
ZM10	7.5(4)	0	105/70	<10	10	<0.1	1	1	10/5	1	<1	<5	10
		1	19,19(5)	<10	7	<0.1	<1	1	2	1	<1	<5	10
		3	21,20	<10	7	<0.1	<1	1	2	1	<1	<5	10
		5	40,37	<10	5	<0.1	<1	1	2	1	<1	<5	10
		7	78,69	<10	5	<0.1	<1	1	2	1	<1	<5	15
		9	109,100	10	7	0.3	1	1	7	1	<1	<5	30
		11	187,186	<10	7	2	5	1	30	200	<1	7	100

Rods were 10" long and 0.625" in diameter, fabricated from same billet and melted in a vacuum in an Al_2O_3 boat with a MgO wash.

(1) 15 passes at 15" per hour.

(2) "0," analysis in ppm before melting.
"1," start of first zone,
"3," start of third zone, etc.
"11," end of rod.

(3) Analysis at leading and trailing ends of rod.

(4) 5 passes at 1" per hour, 15 passes at 7.5" per hour.

(5) Check analysis at same location.

2. Siliconizing of Uranium (C. Marzano, R. A. Noland)

Diffusion coatings (βUSi_2) of silicon in uranium have been produced by immersing uranium specimens in hot NaK alloy containing dissolved silicon metal.

Coating thickness increases with increasing silicon concentration, temperature, and time. Heavy coatings crack and have a strong tendency to spall. Adherent coatings have been reproducibly produced when the coating variables have been adjusted for the production of thin layers.

The corrosion resistance in boiling distilled water has been disappointing. Some improvement is shown during the first few hours of test, but local pinhole attack soon permits undercutting with consequently large losses in weight, and the ultimate loss of the coating.

3. Thermal Cycling of Canned Uranium Slugs (K. F. Smith, H. H. Chiswik)

To determine the can thicknesses of stainless steel necessary to restrain deformation of uranium slugs cycled into the gamma region, eight capsules were made with a wide range in wall thicknesses. Slugs of beta treated uranium, 3/8" in diameter and 1" long, were wrapped in zirconium foil and enclosed in Type 347 stainless steel cans with wall thicknesses varying from 0.013" on the thinnest to 0.047" on the heaviest capsule. The ratio of clad to core cross sectional area here represented is a range of about 15 to 60%. The wrapping in zirconium foil served to avoid reaction with the stainless steel which would otherwise occur at the high cycling temperatures. The excess volume in the cans is estimated at 6% and was sufficient to allow the slugs to be free and "rattle" prior to cycling.

Lines carefully scribed on the outside surface of each capsule allowed 22 separate measurements of length and diameter at different points by means of a microscope comparator. Although changes in dimensions of 1% should be readily measured by this means, after 150 cycles in a sodium autoclave from 100° to 800°C, no deformation as great as 1% has been observed. After 15 cycles, it was observed, however, that the slugs were no longer free to move. In this test, the heating time is approximately three minutes, the cooling time approximately sixteen minutes, and the holding time at temperature is zero.

4. Effect of Irradiation Upon Uranium-Zirconium Alloys (J. H. Kittel, F. Pausche, R. J. Fousek, S. H. Paine)

Irradiations in the MTR of 10% enriched uranium alloys containing 1 and 2 w/o zirconium have continued, and total atom burnups as high as 5.3% (45,000 MWD/T) have been produced in specimens returned for examination.

Observations have been limited, however, to specimens which have shown promise, based on earlier irradiations. Of these, the cast 2% alloy appears to be best. In Figures 13 to 15 are shown specimens of this material examined this quarter, and it can be noted that relatively good surface smoothness and dimensional behavior are shown by this material. Figure 16 summarizes the effect of irradiation on the lengthwise dimensions of specimens of the cast alloy, and in Figure 17 are shown density changes. It is of interest that the cross section of the specimens increased at almost the rate of the length change, indicating that the growth rate is resulting largely from inherent volume changes due to the accumulation of fission products in the lattice.

5. Cooperative Study Between ANL-BMI-KAPL on Stabilized Uranium (J. H. Kittel, F. Pausche, R. J. Fousek, S. H. Paine)

Irradiations were begun this quarter on uranium alloys containing 1 and 2 w/o Zr, 0.1 and 0.4 w/o Cr, and on unalloyed uranium supplied by BMI and KAPL. Sufficient data have not yet been obtained to evaluate the alloys, but early results disclosed an unexpected irradiation effect. The as rolled and annealed uranium-zirconium alloys containing normal amounts of carbon (100 to 500 ppm) had been found to show exceptionally large growth coefficients on thermal cycling, up to 1200 microinches per inch per cycle. Under burnups of at least 0.04%, however, the material was found to shorten under irradiation, at rates of about 150 microinches per inch per ppm burnup. Other preliminary data on both the zirconium and chromium alloys indicate a lack of correlation between thermal cycling and irradiation dimensional changes.

6. Effect of Irradiation Upon Uranium-Niobium Alloy (J. H. Kittel, F. Pausche, R. J. Fousek, S. H. Paine)

Recent work by J. E. Draley has shown that gamma quenched uranium alloy containing 3 w/o Nb has relatively good resistance to corrosion by hot water (ANL-5078). In order to determine the effect of irradiation on rolled and heat treated material, a group of specimens was irradiated in the MTR to total atom burnups up to 0.15%. Figure 18 shows a typical specimen after irradiation. The appearance of the specimen before irradiation is similar to that shown in Figure 13. As can be noted, this alloy is unstable in the rolled and heat treated condition. Based on results obtained with other alloys, castings would probably show better dimensional stability under irradiation.

7. Effect of EBR Irradiation Upon Type 347 Stainless Steel (W. F. Murphy, S. H. Paine, A. C. Klank)

Some of the modified Type 347 stainless steel material used in construction of the Experimental Breeder Reactor was fabricated into tensile specimens which were intended to monitor the radiation damage history of

Figure 13. Appearance of a Typical Uranium Alloy Specimen Before Irradiation.

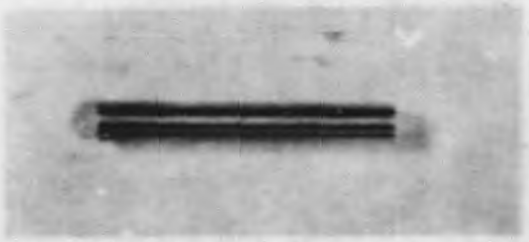

Macro #14625 2-X

Figure 14. Effect of 1.6% Total Atom Burnup (14,000 MWD/T) on Cast 2 w/o Zirconium-Uranium Alloy. Calculated Maximum Irradiation Temperature, 230°C.

Macro #15393 2-X

Figure 15. Effect of 2.3% Total Atom Burnup (20,000 MWD/T) on Cast 2 w/o Zirconium-Uranium Alloy. Calculated Maximum Irradiation Temperature, 330°C.

Macro #15392 2-X

Figure 16. Effect of Irradiation on the Dimensions of Cast 2% Zirconium–Uranium Alloy Specimens.

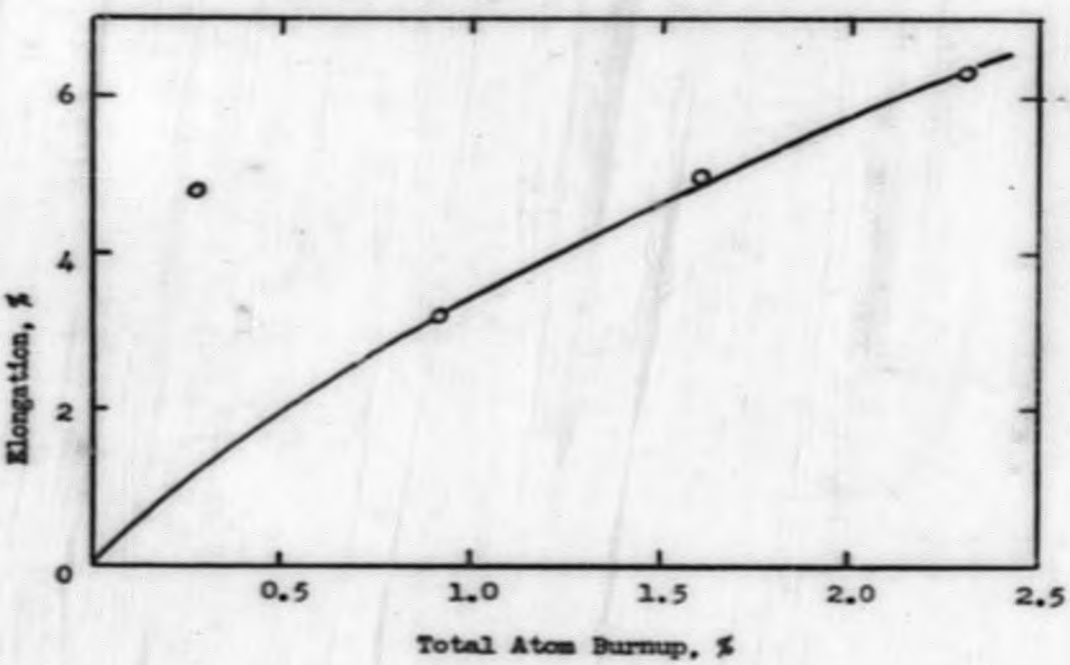

Figure 17. Effect of Irradiation on the Density of Cast 2% Zirconium-Uranium Alloy.

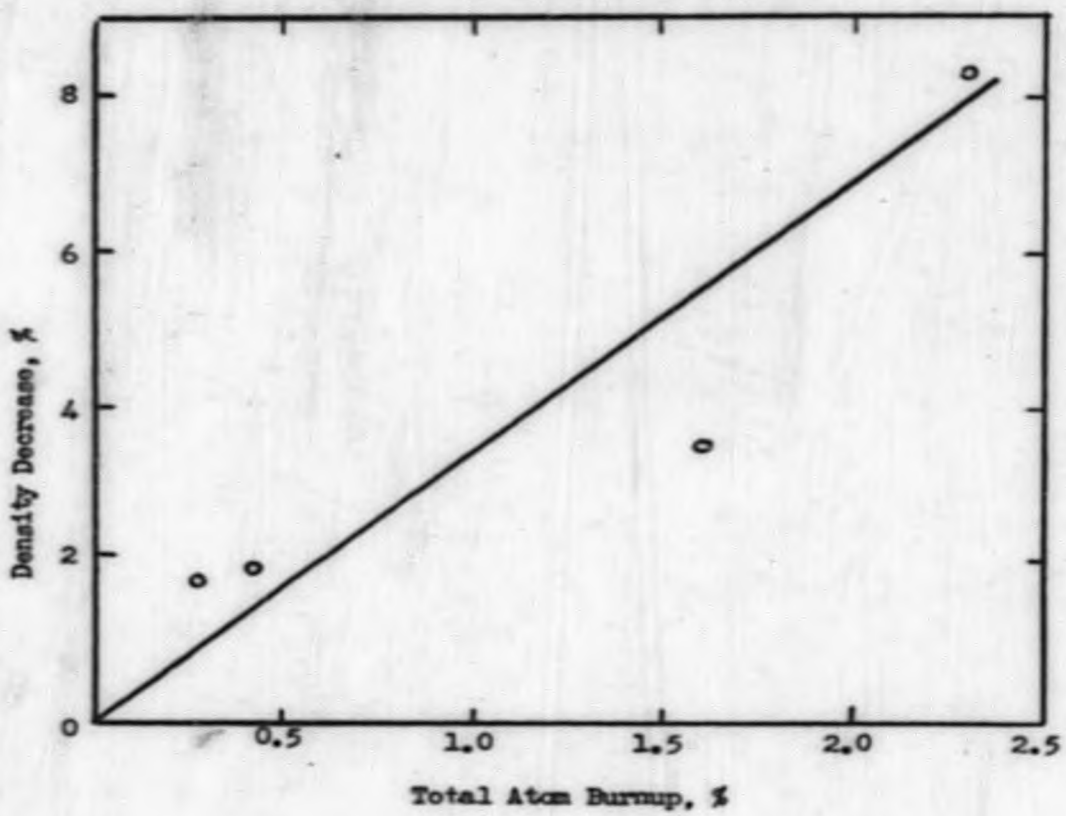

Figure 18. Effect of 0.15% Total Atom Burnup (1,300 MWD/T) on Rolled and Gamma Quenched 3 w/o Niobium-Uranium Alloy. Calculated Maximum Irradiation Temperature, 190°C.

Macro #15432 2-X

the structural material of the reactor. In order to obtain data on a vertical traverse of fuel and upper and lower blanket regions, and to observe the progressive changes in properties due to flux and temperature gradients, a special notched specimen design was developed. The notches are circumferential grooves spaced every 5/8" along a thin cylindrical rod 0.130" in diameter. Notch radius is 0.010", and diameter of the gauge formed is 0.095". Eighteen of these specimens in a hexagonal array fill a rack in a dummy fuel rod which is perforated to allow the reactor NaK to act as a heat transfer medium. In a complete traverse of the specimens, 27 tensile values may thus be obtained, no two of which are subjected to the same temperature and flux conditions.

Irradiation of these specimens took place at the outer edge of the reactor fuel core. Tests have been run after various intervals which have integrated a fast neutron flux as high as 2.4×10^{20} nvt. It was anticipated that the maximum induced hardness and tensile strength changes in the material would not coincide with the flux maximum because of temperature rise in the pile coolant during traverse of the fuel. Data show this to be true, maximum hardening occurring in the lowest quarter of the fuel length where temperature is at a minimum.

The maximum hardening effect at approximately 230°C and at 1.8×10^{20} nvt has increased the tensile strength 17,000 psi and the hardness 4 Rockwell A points for each tenfold increase in exposure. A plot of property versus log nvt is linear, tending toward saturation but not having reached it as yet. A comparison of the hardness behavior with work reported by Bowman[7] on SS-347 bombarded by 38 Mev alpha particles at -100°C shows a surprising empirical agreement which, if real, indicates that saturation may occur at 10^{21} nvt.

---

[7] NAA-SR-287, F. E. Bowman et al, "Cyclotron Irradiation Damage of Thorium, Stainless Steel and Zirconium," April 1, 1954.

VI. AQUEOUS CORROSION

1. Corrosion of Aluminum in Dilute Aqueous Solution (J. E. Draley, N. Williams)

Examination of new data, available since the last quarter, has resulted in a change in our opinion concerning what is indicated for the phenomena taking place during the initial stages of the corrosion of aluminum in distilled water. In the last Quarterly Report (ANL-5234) it was stated that approximately one-tenth of the corrosion product was continuously lost to the solution. This is no longer believed to be true but rather than a considerable fraction of the product of corrosion is lost to the solution in the first half-hour of exposure. Subsequent to that time no measurable amount of corrosion product is lost. It is indicated that at least one-third of the corrosion product which is formed in the first half-hour does not remain on the sample surfaces. Further corroboration of the point and more quantitative information will be forthcoming. The reactions taking place will undoubtedly be important in explaining the rather large amount of corrosion which takes place during the initial exposure period of aluminum, even though the ultimate corrosion rate may be quite low.

2. High Temperature Aqueous Corrosion of Aluminum (J. E. Draley, W. E. Ruther)

Tests reported last month at 250° and 275°C with potassium dichromate and sodium silicate as inhibitors at a pH of 3.5 have been concluded. At both temperatures an intergranular attack set in before the termination of the tests. The silica addition was apparently successful in delaying the onset of such attack over what would have been observed in its absence, but did not eliminate it. It has consistently been believed that metal which suffers this type of attack is unsatisfactory for a practical application. Although relatively low concentrations of sodium metasilicate are observed to delay such attack, it is not believed desirable at this time to investigate the addition of greater concentrations. At 100 ppm SiO_2 the test systems became plugged by the deposition of a silicaceous material.

In the initial stages in the intergranular attack of aluminum in water and dilute solutions, small blister-like protuberances are formed on the metal surface. These usually consist of a mixture of aluminum and aluminum oxide when examined. Continued exposure of the samples to the environment causes a rapid increase in effective corrosion and samples rapidly lose strength. It is suggested that this blistering attack occurs through the following sequence of events.

A proton penetrates the protective oxide layer and is reduced at the aluminum metal surface (local cathode). As atomic hydrogen it can then either diffuse back through the film or into the aluminum metal, depending on the temperature, film thickness and porosity. If the metal contains any internal cavities, the atomic hydrogen diffusing into these cavities combines to form hydrogen gas under pressure. The strength of aluminum is low at the temperatures considered; thus the metal yields and a bulge is formed on the surface. When this blister breaks, water is admitted to fresh metal, producing more hydrogen, and the process is self-accelerating.

Assuming that this explanation is correct, there are at least two methods of retarding or eliminating this type of accelerated corrosion. One is to provide "local cathodes" of a material (preferably of low hydrogen overvoltage so that nearly all hydrogen formed will be at such cathodes), located so the liberated hydrogen is free to diffuse away into the electrolyte. The other method is to provide aluminum metal which is essentially rift or cavity free.

Simple experiments were performed to test these methods. To provide "local cathodes" other than the aluminum metal, reducible metal ions were added to the test medium. Fifty parts per million solutions of various cations were adjusted to the same pH using sulfuric acid or potassium hydroxide. Freshly prepared 2S aluminum sheet samples were corroded for 48 hours in the degassed solutions at 300°C. The results obtained are shown in Table VIII.

The appearance of the samples correlated with the weight change data. The specimens with small weight changes had smooth, adherent films over most of the surface with isolated microscopic dendritic growths of a material which glistened in a metallic fashion under the microscope. The appearance of these growths formed in nickel sulfate solution is shown in Figure 19. No blistering was evident on the samples in Co^{++}, Cd^{++}, and Ni^{++} solutions. This protection from blistering was not a short time effect. A sample was tested in 50 ppm Co^{++} solution at pH 3.0 for 24 days at 300°C. At the end of the test period the only blistering in evidence was around a support hole, drilled after the sample had been annealed. The total weight gain for the period was 2.2 mg/cm^2 of which about half was acquired in the first four days.

Based on these preliminary results, long time corrosion rate studies were started using nickel ion. A test of 50 ppm Ni^{++} - pH 3.5 - 275°C was abruptly terminated when a preheater tube plugged with a hard precipitate (as yet unidentified). Another test using 5 ppm Ni^{++} (no pH adjustment) has been operating for 15 days. Unfortunately, an error in setting the temperature controlling equipment resulted in operation at 208°C, so that the excellent behavior observed is not good evidence of the effectiveness of the nickel ion.

Another way to prevent the formation of hydrogen at the sample surface is to make the entire sample anodic by an external polarizing current. This experiment was performed in a large autoclave with electrical leads. A 20 $\mu a/cm^2$ polarizing current was applied between the sample and a stainless steel counterelectrode. One anodic, one cathodic and one control (no current) samples were tested 4 hours at 325°C in degassed distilled water. The amount of aluminum corresponding to the electricity passed is a trivial part of the weight change.

The results were in accord with the proposed mechanism. The blistering was essentially eliminated (except for a few, small ones - maximum height, 0.003") on the anodic sample. In this case the cathodic reaction (hydrogen) was assumed to take place at the stainless steel counterelectrode. With the current reversed, several strings of large protuberances about 0.060" maximum height, as well as several isolated blisters formed. The control sample had four large blisters and thus was intermediate between the anodic and cathodic.

The second suggested method of blister elimination (sound metal) has been partially investigated. A piece of 2S aluminum was vacuum melted (10^{-5} mm, 700°C) and cooled slowly through the solidification temperature. One piece of this ingot (a cube 1 x 1 x 1 cm) was compressed flat in a testing machine by a 100,000 pound load. This was done to provide a cold worked sample. A comparison test of the vacuum cast, compressed and control 2S samples was made in distilled water at 300°C. The weight gains are shown in Table IX.

In Figure 20 are shown the surfaces of the 2S control specimen at the end of the 66 hour test, and of one side of the vacuum cast specimen after 132 hours exposure. The bulk of the latter surface was a much lighter grey than the 2S control. Note the segregation of impurities and the absence of blistering. On much of the other side of the same sample the segregated impurities resulted in the formation of numerous pits. Judging by the color, the material corroded in these areas was rich in iron. The over-all appearance of the compressed specimen was very similar to the as cast sample, but the surface showed a large number of small blisters.

Certain other exploratory experiments have been performed. One series consisted of short term tests in which 2S aluminum sheet samples were used and the pH varied to determine the range of minimum attack. The results in Table X indicate that at temperatures in the range 200° to 300°C the least attack (for short exposures) occurred at pH 3. Note that when potassium sulfate was added in quantities sufficient to have the sulfate ion concentration equal to that of a pH 3 sulfuric acid solution, relatively little difference in corrosion from that in distilled water was observed.

A test using high purity aluminum was performed to determine if the attack proceeded by blistering in the absence of impurities. The test was performed at 160°C in degassed distilled water. By 43 hours the sample showed ridges of mixed oxide and metal with occasional bulges open at the top, like miniature volcanoes. This continued to be the pattern of corrosive attack. By the end of 139 hours the oxide coating was very heavy. Some flakes of oxide were noted in the autoclave and more could be removed by gentle brushing of the sample. In the early examinations the coating on the sample was dark grey. By 139 hours the oxide on the specimen was lighter in color and the flaked off oxide was completely white. The results are thus in line with those of other investigators (notably LaVigne at Chalk River) who report increasing susceptibility to intergranular attack with increasing metal purity.

TABLE VIII

Corrosion of 2S Aluminum at 300°C

Solution*	Weight Gain (mg/cm^2) in 48 Hour Test	Comments
50 ppm Co^{++} pH 4	0.74	Blue film, no
pH 7	0.66	blisters.
50 ppm Cd^{++} pH 4	0.60	Light blue, no
pH 7	0.78	blisters.
50 ppm Ni^{++} pH 4	0.76	No blisters, light
pH 7	0.93	grey.
50 ppm Sn^{++} pH 4	0.91	Few microscopic blisters.
pH 7	No Test (Precipitate formed)	
50 ppm Cu^{++} pH 4	0.95	Few microscopic blisters.
pH 7	No Test (Precipitate formed)	
50 ppm Pb^{++} pH 4	2.68	Dark grey, few
pH 7	1.12	blisters.
pH 4 H_2SO_4	3.1	Control specimens, both
H_3PO_4	4.3	badly blistered.

*Solutions were made up using the sulfate of the required cation except for $Pb(NO_3)_2$.

TABLE IX

Corrosion of 2S Aluminum at 300°C in Degassed Distilled Water

Sample	Weight Increase (mg/cm^2) in 66 Hours	Comments
Vacuum Melt - As Cast	1.9	No blisters
Vacuum Melt - Compressed	2.5	Few small blisters.
2S Control	7.5	Badly blistered.

TABLE X

Corrosion of 2S Aluminum as a Function of pH.
Aluminum Metal Corroded, mg/cm^2

pH (H_2SO_4)	200°C 48 Hours	250°C 20.5 Hours	300°C 6 Hours
2	1.3	0.59	0.51
3	0.16	0.07	0.19
4	0.18	0.36	0.23
5	0.25	0.42	0.36
6.5	0.25	0.47	0.60*
(Distilled)			
6.3	$SO_4^=$ conc. = pH 3 H_2SO_4		0.57

*Calculated from weight gain - sample could not be effectively stripped due to blisters.

Figure 19. Nickel Growth on 2S Aluminum at 300°C.

Exposure: 48 hours in $NiSO_4$ (50 ppm Ni^{++}), adjusted to pH 7.

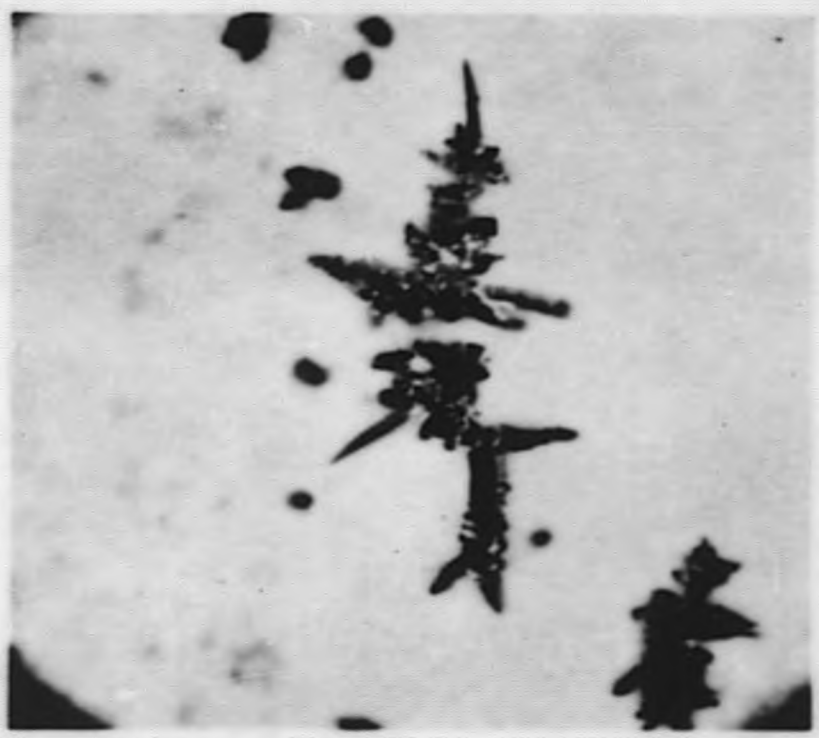

Micro #15446 250-X

Figure 20. 2S Aluminum After Exposure to Distilled Water at 300°C.

Top: Commercially rolled metal, after 66 hour test
Bottom: Vacuum melted metal, after 132 hour test

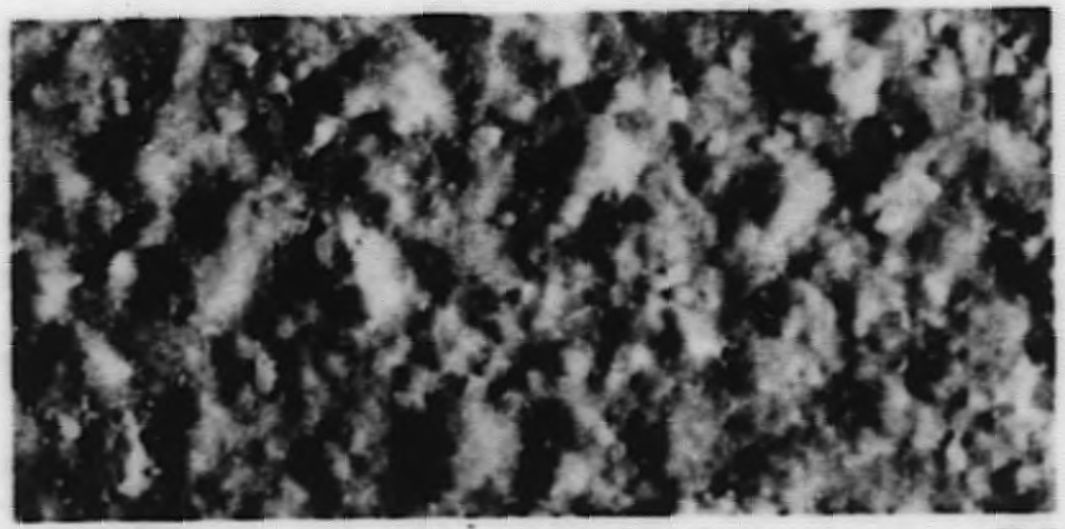

Macro #15438 20-X

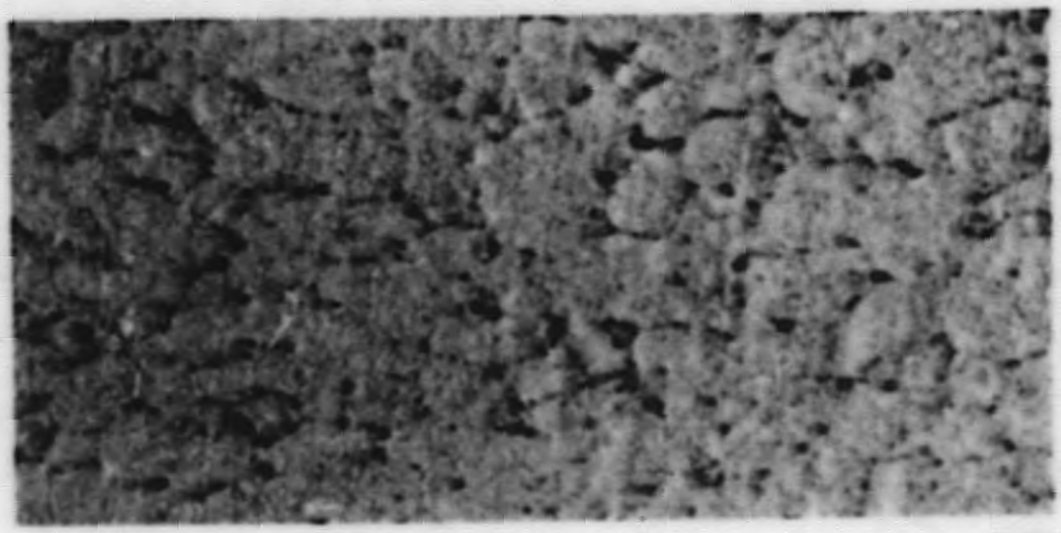

Macro #15439 20-X

3. Mechanism of the Aqueous Corrosion of Zirconium (R. D. Misch)

One of the possible ways that the oxide film formed on zirconium in water can limit the corrosion rate is by providing a high resistance to the necessary passage of electrons through it from the metal to the solution interface. Attempts to measure the resistance of such films on pieces of zirconium have been made by immersing suitably prepared samples in mercury and measuring d.c. voltage-current relationships.

The resistance was found to increase with decreasing current density with indication of some sort of breakdown above 0.02 $\mu a/cm^2$. Further study of the phenomena involved in the dependence of resistance on current density is under way.

Anodic films were applied to several samples in two standard thicknesses: one in which the anodizing voltage was increased to 2 volts and held, the other in which the voltage applied was 50 volts. The anodizing solution was 1 w/o KOH solution at room temperature. This method of applying films can be regarded as one which can reproducibly provide films of known thickness. The data of one series of measurements are given in Table XI.

The samples from the bottom of the ingot, which were examined first, showed a large variation in resistance which appeared to correlate with corrosion resistance. However, this relationship now appears to have been fortuitous. Two further sets of data were obtained under the same conditions and the correlation was not produced. If those measurements which indicate zero resistance (believed due to one or more defects in the film) are discarded, the average of the remaining resistances is approximately 950 $ohms/cm^2$ of the exposed surface for the anodized films applied at 2 volts, as well as those applied at 50 volts. It is evident that the thicker film did not proportionally increase in resistance, as would be expected from an ohmic conductor.

It is believed either that only a thin portion of the film was acting as a barrier, or that dielectric breakdown was occurring. If the second hypothesis is correct, then a true measure of resistance can only be found at current densities low enough so that the voltage across the film does not exceed the breakdown voltage. Experiments were therefore conducted at 0.018 $\mu a/cm^2$ for specimens with a 2 volt film. Again no particular correlation was found with corrosion resistance of the samples. In this case the average resistance was found to be 1.4×10^7 $ohms/cm^2$. It is interesting that the resistance observed is the right order of magnitude to be a limiting factor in the corrosion rate.

TABLE XI

Comparison of the Electrical Resistance of Films Produced Anodically with Corrosion Rates for Eight Zirconium Specimens (d.c. Resistance at 170 $\mu a/cm^2$)

Specimen Designation		Wt. Gain After 2 Weeks in Water at 300°C (mg/cm^2)	Appearance	Resistance of the Film (in Kilohms/cm^2) As Applied at the Indicated Anodizing Cell Voltage	
				2V	50V
2	T*	1.2	All White	0.17	1.1
	B	20.4	All White	0.03	0.45
3	T	0.05	Interference Colors	0.67	0.85
	B	0.09	Interference Colors	5.2	5.9
4	T	0.08	Slight White Areas	0.14	0.14
	B	0.07	Slight White Areas	1.3	0.14
5	T	0.19	White Areas	0.3	0.56
	B	0.12	White Areas	0.53	0.56

*Indicates the top of ingot No. 2; B indicates the bottom; similarly for the others.

4. Aqueous Corrosion of Magnesium (R. D. Misch)

Four tests have been run at 90°C in recirculating systems in which magnesium alloys have been exposed to dilute alkaline solutions. In all cases four samples were placed in the glass sample holders and removed one at a time. Each sample was then stripped of corrosion product in hot chromic acid solution. The weights of the amount of metal corroded for the various exposure times were thus available. In all tests the potassium hydroxide solution was made up to pH 10.0, since tests at lower temperatures had indicated this to be the pH of the solution which magnesium will maintain by the corrosion process. In the first two tests, no special provision was made to maintain the pH of the solution. A small amount of solution was added as required to maintain the water level in the system. In these cases the pH diminished rather rapidly for the first several days and then more slowly, reaching a value of the order of 8.2 at the end of the twenty-day test. Data for these tests are shown as the bottom two curves in Figure 21. Two alloys were tested; one the commercial FS-1a alloy, which contains typically 2.7% aluminum, 0.3% manganese, 1.0% zinc. The other alloy used was a special AEC high purity aluminum alloy of magnesium. It contained 2.7% aluminum, and all other impurities were held at an unusually low level. It is observed that corrosion increased with time of exposure for both alloys. The difference in behavior between the two is unimportant.

The test was repeated for alloy FS-1a with the small continuous addition of fresh solution in an effort to maintain original pH. It was suspected that the drop in pH in the first tests was due to air leakage into the system. In this case the solution pH diminished from 10.0 to about 9.7, and in this case the flow rate was 17 feet/second as compared to 20 feet/second in the first two tests. The data are presented as one of the top curves in Figure 21, along with a fourth test in which the solution was saturated with helium to provide an essentially oxygen-free test. Apparently there was no significant difference between the behavior of the samples in oxygen-saturated solution and that in helium-saturated solution. Corrosion rates subsequent to the first ten days were of the order of 15 mg/dm^2/day at pH slightly below 8.5 and 20 feet/second; 25 mdd at pH 9.7 and 17 feet/second flow rate.

One test was performed at 150°C under essentially stagnant conditions using pH 10 (KOH) oxygen-saturated solution. The magnesium had disintegrated by the end of four days.

5. The Aqueous Corrosion of Uranium (W. E. Ruther, G. Dragel)

The corrosion rate of natural uranium (Los Alamos Ingot 547) was determined in boiling distilled water after heat treating at 1000°C for six hours in vacuum. A value of 2.8 milligrams/cm^2/hour (mch) was obtained.

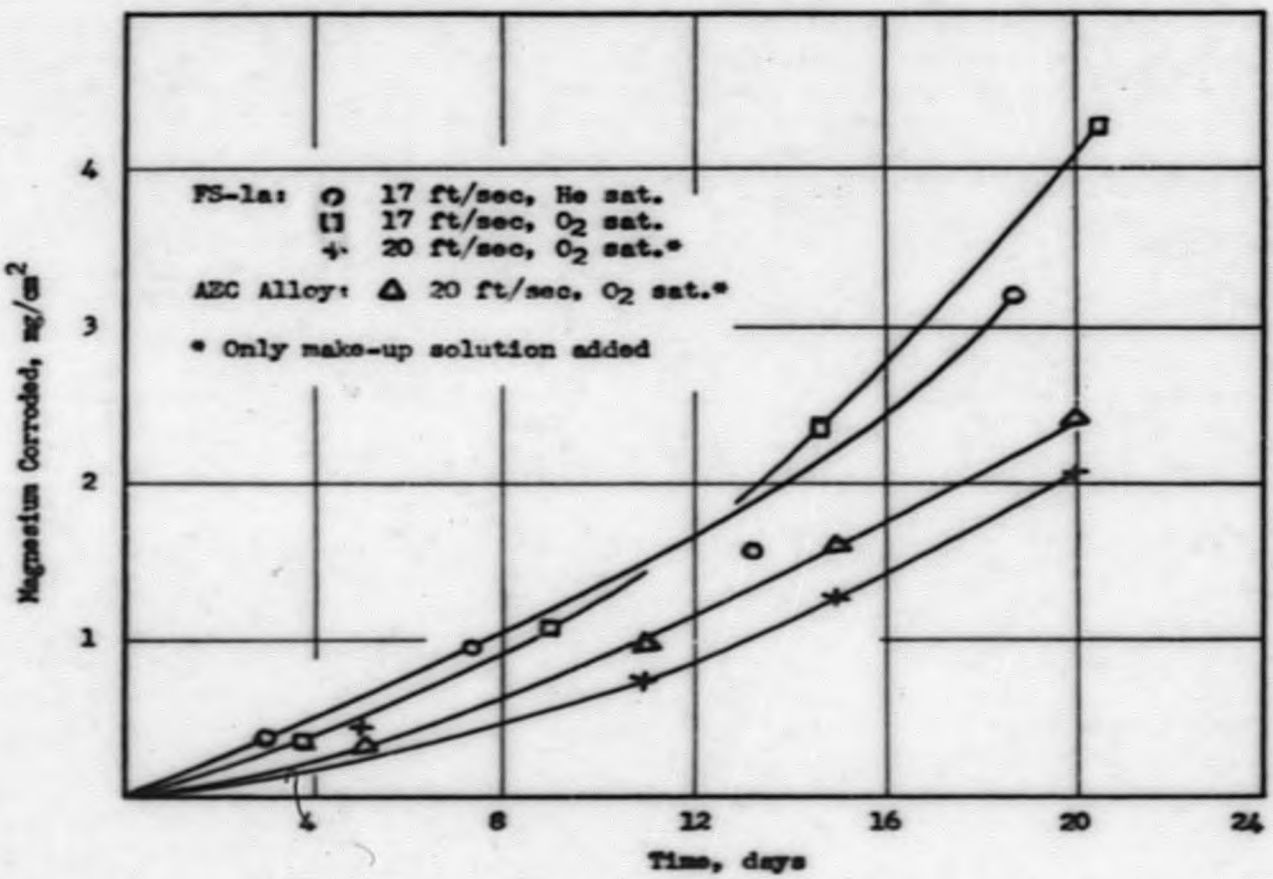

FIGURE 21

CORROSION OF MAGNESIUM IN DILUTE KOH AT 90°C.

This supersedes the value of 1.8 mch tentatively reported last quarter. The difference is the result of treatment of additional data. Last quarter one sample had been corroded for 96 hours, and the rate given assumed linear corrosion from zero time. The new rate was calculated from a plot of three weight losses versus time. A straight line drawn through the data intersected the abscissa at 0.25 days, indicating the length of time required to build up to the steady state corrosion rate.

6. Corrosion Resistant Uranium Alloys (J. E. Draley, W. E. Ruther)

A series of uranium alloys containing nominally 5 w/o zirconium and various amounts of niobium were tested in degassed distilled water at 300°C. All alloys were quenched in liquid Wood's metal after one hour in vacuum at 1000°C. The corrosion observed is shown in Table XII.

TABLE XII

Effect of Niobium Additions to Uranium-5 w/o Zirconium Alloy

Alloy	Average Corrosion Rate (72 Hours in Water at 300°C) mcd(1)
H288 (0.51% Nb + 4.90% Zr)	Disintegrated
H289 (1.06% Nb + 4.85% Zr)	Disintegrated
H290 (1.47% Nb + 4.81% Zr)	14
H311 (2% Nb + 4.80% Zr)	15

All percentages are by weight.

(1) mcd = milligrams/cm^2/day.

It is indicated that more than 1% niobium is required to produce corrosion resistance, and that small additions beyond 1.5% do not improve the corrosion resistance. Previous testing of samples containing amounts of zirconium in the vicinity of 4% with 1-1/2 to 2% niobium has shown an unsatisfactory corrosion resistance. Thus it appears that a minimum of about 5% zirconium and 1-1/2% niobium should be specified to produce an acceptably corrosion resistant alloy.

From the behavior of some old castings in this alloy series, it was suspected that the presence of silicon is deleterious to this type of corrosion resistant alloy. Half of a casting of nominally 1.5% Nb - 5% Zr alloy was

recast with 300 ppm silicon added. From the data in Table XIII, it is clear that this amount of silicon is harmful to this alloy. The concentration of silicon in casting H272 is that normally present as an impurity in the constituents used in making this alloy.

TABLE XIII

Effect of Silicon Addition on the Corrosion of 1.5% Nb-5% Zr Uranium Alloys

As Quenched Alloy	Average Corrosion Rate (72 Hours - 300°C) Milligrams/cm²/day
H272 [1.48% Nb + 4.70% Zr, 0.003% Si]	18
H277 [1.44% Nb + 4.90% Zr, 0.03% Si]	Disintegrated

A series of uranium alloys based on the 3% niobium composition was made containing ternary elements added to the extent of 20% of the atom per cent of niobium in the alloys. The results of the corrosion tests of such materials are shown in Table XIV.

TABLE XIV

Corrosion Test at 300°C in Degassed Distilled Water.

Alloy and Nominal Composition*	Average Rate After Quench from 800°C (mcd)**	Average Rate (Quenched, Then Aged 50 Hours at 350°C) (mcd)
H273 3% Nb	7.4	Disintegrated
H279 3% Nb + 0.18% Si	342	Disintegrated
H281 3% Nb + 0.37% Ni	86	290
H282 3% Nb + 0.74% Sn	25***	19

*H279, 281 and 282 made by adding indicated amounts of Si, Ni, or Sn to H273.

**mcd = milligrams/cm²/day.

***One as quenched piece marked as H282 disintegrated. A sample mixup in machining is suspected since a recheck has given the indicated rate.

An additional alloy containing 0.35 w/o iron was made but not tested since it split on rolling and cracks extended through every usful piece. It is apparent that only the alloy containing tin showed corrosion resistance comparable to that of the basic 3% niobium alloy, and furthermore, that this alloy had considerably more resistance to the harmful effect of aging at elevated temperature than did the niobium binary alloy. A further series of tests was made to investigate the ability of the tin alloy to withstand higher temperature aging. The results are shown in Table XV. Samples of the same rolled casting whose results are described in Table XIV were used in this series of tests. The composition is given as 0.61% tin in Table XV, since chemical analysis showed approximately this value for the top and the bottom of the casting.

TABLE XV

Effect of High Temperature Aging on Corrosion Resistance of Alloy H282 (3% Nb-0.61% Sn)

Aging Treatment*	Corrosion Test (300°C)	
	Time of Test (hours)	Average Rate (mcd)
375°C - 24 hours	73**	17
	139	Essentially Disintegrated
400°C - 24 hours	72	14
	205	14
425°C - 24 hours	72	185

*Specimens first quenched from 1000°C.
**Crack noted in specimen.

The considerable resistance to aging at 400°C is encouraging. It is suspected that this alloy composition possesses the highest degree of resistance to harmful aging yet investigated here. Two things are worth noting. The first is that high temperature aging seems to have reduced the rate of corrosion of the material over that exhibited by samples in the as quenched condition. This phenomenon has also been noted for alloys containing nominally 1.5% Nb + 5% Zr. Its explanation is not known. Secondly it is suspected than the better results from the sample aged at 400°C than those from the sample aged at 375°C are due to differences in the samples themselves. This casting was a small one and there were cracks in some samples before testing. In addition, the tin content might have had some influence. The sample used to

obtain the data after 400°C aging was analyzed and showed 0.71 % tin, higher than the analysis obtained for the two ends of the alloy casting. It is suspected that heterogeneity is indicated and that somewhat higher tin contents are desirable. A new series of alloys has been requested, with varying tin contents.

END